


DESIGN AND SYNTHESIS OF BERBERINE DERIVATIVES  
AS CHOLESTEROL LOWERING AGENT



Presented in Partial Fulfillment of the Requirements for the  
Master of Science Degree in Chemistry  
at Srinakharinwirot University

July 2018

DESIGN AND SYNTHESIS OF BERBERINE DERIVATIVES AS  
CHOLESTEROL LOWERING AGENT




A THESIS  
BY  
METHACHANUN JAITRONG

Presented in Partial Fulfillment of the Requirements for the  
Master of Science Degree in Chemistry  
at Srinakharinwirot University

July 2018

Copyright 2018 by Srinakharinwirot University

DESIGN AND SYNTHESIS OF BERBERINE DERIVATIVES AS  
CHOLESTEROL LOWERING AGENT



AN ABSTRACT  
BY  
METHACHANUN JAITRONG

Presented in Partial Fulfillment of the Requirements for the  
Master of Science Degree in Chemistry  
at Srinakharinwirot University

July 2018

Methachanun Jaitrong. (2018). *Design and Synthesis of Berberine Derivatives as Cholesterol Lowering Agent*. Thesis, M.Sc. (Chemistry). Bangkok: Graduate School, Srinakharinwirot University. Advisor Committee: Assoc. Prof. Dr. Siritron Samosorn, Dr. Pornthip Boonsri

Worldwide, cardiovascular disease has assumed an increasing role as a major cause of morbidity and mortality. Cardiovascular disease is closely related with high cholesterol level. One major method for treating cardiovascular disease is the inactivation of enzymes involved in cholesterol biosynthesis. The target enzymes included 3-hydroxy-3-methyl-glutaryl-CoA reductase (HMGCR) and phosphomevalonate kinase (PMK). Berberine, a natural plant product, can reduce cholesterol level and does not harm people. This study aimed to design the derivatives of berberine in order to inhibit the activities of HMGCR and PMK. The desired berberine derivative were successfully synthesized via Manich, alkylation, demethylation and hydrolysis reactions. The results showed that all derivatives could inhibit HMGCR activity. In particular, compounds **41** and **42** displayed a promising inhibitory effect on HMGCR by 12-fold higher activity than that of berberine. In addition, They showed stronger binding interaction with PMK at  $K_d$  values of  $64.77 \pm 4.80$  and  $85.09 \pm 6.84$   $\mu\text{M}$ , respectively, which better than that of berberine ( $190.60 \pm 17.86$ ) 2.2–2.9 folds. Considering, substitution of naphthalenylmethyl at position C-13 and alkoxy carboxylic substituents at the C-9 position of berberine which had a significant effect on the inhibition of target enzyme activities. Therefore, compounds **41** and **42** are good leads for the development of novel compounds that effective in inhibiting the activities of HMGCR and PMK.

การออกแบบและการสังเคราะห์อนุพันธ์เบอร์เบอร์นให้เป็นสารที่มีฤทธิ์ระดับคอเลสเตอรอล



เสนอต่อบัณฑิตวิทยาลัย มหาวิทยาลัยศรีนครินทรวิโรฒ เพื่อเป็นส่วนหนึ่งของการศึกษา  
ตามหลักสูตรวิทยาศาสตรมหาบัณฑิต สาขาวิชาเคมี

กรกฎาคม 2561

เมธาชนันท์ ใจตรง (2561). การออกแบบและสังเคราะห์อนุพันธ์เบอร์เบอร์อินให้เป็นสารที่มีฤทธิ์ลดระดับคอเลสเตอรอลปริณยานิพนธ์. วท.ม. (เคมี). กรุงเทพฯ: บัณฑิตวิทยาลัย มหาวิทยาลัยศรีนครินทรวิโรฒ. อาจารย์ที่ปรึกษาปริณยานิพนธ์ : รองศาสตราจารย์ ดร.สิริธร สโมสร, ดร. พรทิพย์ บุญศรี

ในปัจจุบันมีอัตราของผู้ป่วยและผู้เสียชีวิตจากโรคหัวใจและหลอดเลือดสูงขึ้นอย่างต่อเนื่องและมีแนวโน้มเพิ่มมากขึ้นเรื่อยๆ ทั้งนี้มีสาเหตุสำคัญมาจากการมีระดับคอเลสเตอรอลในเลือดสูง แนวทางหนึ่งที่จะช่วยลดภาวะคอเลสเตอรอลสูงในเลือด คือ การยับยั้งเอนไซม์บางตัวที่ใช้ในการสังเคราะห์คอเลสเตอรอลในวิถีการสังเคราะห์คอเลสเตอรอลในร่างกาย เอนไซม์ที่เป็นเป้าหมายคือ 3-hydroxy-3-methyl-glutaryl-CoA reductase (HMGCR) และ phosphomevalonate kinase (PMK) เบอร์เบอร์อินเป็นสารผลิตภัณฑ์ธรรมชาติที่มีสรรพคุณลดคอเลสเตอรอล และไม่มีความเป็นพิษต่อคน ดังนั้นงานวิจัยนี้จึงนำเบอร์เบอร์อินมาใช้เป็นสารต้นแบบ (lead) ในการออกแบบและสังเคราะห์ปรับเปลี่ยนโครงสร้างเพื่อยับยั้งเอนไซม์ HMGCR และ PMK สารอนุพันธ์เบอร์เบอร์อินที่ต้องการสามารถสังเคราะห์ได้โดยเกิดผ่านปฏิกิริยา Mannich, alkylation, demethylation และ hydrolysis ผลการทดลองพบว่าสารอนุพันธ์ทุกตัวสามารถยับยั้งเอนไซม์ HMGCR ได้ โดยเฉพาะสาร **41** และ **42** สามารถแสดงผลที่ดีในการยับยั้งเอนไซม์ HMGCR ซึ่งดีกว่าสารตั้งต้นเบอร์เบอร์อินถึง 12 เท่า นอกจากนี้ สาร **41** และ **42** ยังสามารถจับกับเอนไซม์ PMK ได้ดี ซึ่งมีค่า  $K_d$  ในช่วง  $64.77 \pm 4.80$  และ  $85.09 \pm 6.84$ , ตามลำดับ ซึ่งดีกว่าเบอร์เบอร์อิน ( $190.60 \pm 17.86$ ) 2.2 – 2.9 เท่า เมื่อพิจารณาโครงสร้างพบว่าการแทนที่ด้วยหมู่ naphthalenylmethyl ที่ตำแหน่ง C-13 และการแทนที่ด้วยหมู่ alkoxy carboxylic ที่ตำแหน่ง C-9 ของเบอร์เบอร์อินมีผลต่อการยับยั้งการทำงานของเอนไซม์เป้าหมาย ดังนั้น สารประกอบ **41** และ **42** จึงเป็นโมเลกุลต้นแบบที่ดีในการนำมาพัฒนาสารตัวใหม่ที่มีประสิทธิภาพในการยับยั้งการทำงานของเอนไซม์ HMGCR และ PMK

The thesis titled

“Design and Synthesis of Berberine Derivatives as Cholesterol Lowering Agent”

by

Methachanun Jaitrong

has been approved by the Graduate School as partial fulfillment of the requirements for the  
Master of Science degree in Chemistry of Srinakharinwirot University.

..... Dean of Graduate School

(Asst. Prof. Dr.Chatchai Ekpanyaskul, M.D.)

July , 2018

Thesis Committee

Oral Defense Committee

..... Major-advisor

(Assoc. Prof. Dr. Siritron Samosorn)

.....Chair

(Assoc. Prof. Dr. Boon-ek Yingyongnarongkul)

.....Co-advisor

(Dr. Pornthip Boonsri)

.....Committee

(Assoc. Prof. Dr. Sunit Suksamrarn)

.....Committee

(Assoc. Prof. Dr. Siritron Samosorn)

.....Committee

(Dr. Pornthip Boonsri)

## Acknowledgements

Foremost, I would like to express my sincere gratitude to my research advisor Assoc. Prof. Dr.Siriron Samosorn for the continuous support of my master degree study and research. I am very grateful for her patience, motivation, enthusiasm, and immense knowledge. I could not have imagined having a better advisor and mentor for my study. I also would like to acknowledge my co-advisor, Dr.Pornthip Boonsri for her valuable guidance and suggestions an molecular docking and enzyme assay testing. In addition, I feel grateful to Assoc. Prof. Dr.Ramida Wattanapoleasin and Ms.Patamapan Tamvapee for their biological specialist aspect, and carrying on the enzyme inhibitory activity testing.

Besides my advisors, I would like to thank the rest of my thesis committee: Assoc. Prof. Dr.Sunit Suksamrarn, and Assoc. Prof. Dr.Boon-ek Yingyoungnarongkul, for their encouragement, insightful comments, and hard questions.

I also would like to thank to the Center of Excellence for Innovation in Chemistry (PERCH-CIC) for partially financial support. I am indebted to Department of Chemistry, Faculty of Science, Ramkhamhaeng University for recording the mass spectra.

Many special thanks also go to my lecturers, friends, colleagues and staff of the Department of Chemistry, Faculty of Science, Srinakharinwirot University for their friendship, kind support and encouragement.

Last but not the least, I would like to thank my family for your kindness, love and support to me spiritually throughout my life.

Methachanun Jaitrong

# TABLE OF CONTENTS

Chapter	Page
<b>1 INTRODUCTION</b> .....	1
Background.....	1
Molecular Docking.....	2
Objectives of the research.....	3
<b>2 REVIEW OF LITERATURE</b> .....	4
Cholesterol.....	4
Biosynthesis of cholesterol.....	4
Berberine.....	7
Biological activities of Berberine and berberine derivatives.....	7
3-Hydroxy-3-methyl-glutaryl-CoA reductase (HMG-CoA reductase).....	12
Phosphomevalonate Kinase (PMK) .....	18
<b>3 EXPERIMENTAL</b> .....	21
General Instrument.....	21
Chemical.....	21
Method.....	22
Molecular docking of PMK.....	22

## TABLE OF CONTENTS (continued)

Chapter	Page
<b>3 Continue</b>	
Molecular docking of HMGCR.....	23
Synthesis of Berberine derivatives.....	25
Synthesis of compound <b>9</b> .....	25
Synthesis of compound <b>10</b> .....	26
Synthesis of compound <b>35</b> .....	26
Synthesis of compound <b>36</b> .....	27
Synthesis of compound <b>37</b> .....	27
Synthesis of compound <b>38</b> .....	28
Synthesis of compound <b>39</b> .....	28
Synthesis of compound <b>40</b> .....	29
Synthesis of compound <b>41</b> .....	29
Synthesis of compound <b>42</b> .....	29
Synthesis of compound <b>43</b> .....	30
Synthesis of compound <b>44</b> .....	30
Enzymes Activity.....	31
Phosphomevalonate kinase.....	31
3-Hydroxy-3-methyl-glutaryl-CoA Reductase Inhibition Assay.....	33

## TABLE OF CONTENTS (continued)

Chapter	Page
<b>4 RESULTS AND DISCUSSION</b> .....	34
Synthesis.....	39
Bioassays.....	44
Inhibitory activity of BBR derivatives againsts HMGCR.....	44
Binding Affinity of BBR Derivatives to Phosphomevalonate Kinase....	45
Cholesterol Lowering Agent Studies.....	48
<b>5 CONCLUSION</b> .....	53
<b>REFERENCES</b> .....	55
<b>APPENDIX</b> .....	59
<b>GLOSSARY</b> .....	63
<b>VITAE</b> .....	78

## LIST OF TABLE

Table		Page
1	Inhibitory rate of 8-alkyl-berberine against HMGR and their LD <sub>50</sub> .....	10
2	Structures of potential PMK inhibitors <b>7-10</b> .....	20
3	Reaction volumes for 96 well plate samples.....	33
4	Binding energy of berberine and its derivatives interacted to HMGCR and PMK based on molecular docking).....	35
5	Binding energy of the berberine derivatives ( <b>35-44</b> ).....	38
6	Reaction conditions and % yields for the synthesis of BBR derivatives ( <b>35-39</b> ).....	41
7	Reaction conditions and obtained % yields for the synthesis of BBR derivatives ( <b>40-44</b> ).....	43
8	Fluorescence study was used to experimentally verify binding affinity.....	48

## LIST OF FIGURES

Figure		Page
1	Structure of Berberine.....	2
2	Biosynthesis of cholesterol.....	6
3	Structure of 8-alkylberberine derivatives.....	10
4	Structure of berberine-baicalein (BBS).....	11
5	Structure of <b>4A</b> , <b>4B</b> and <b>4C</b> .....	12
6	Lactone ( <b>4</b> ) and acid ( <b>5</b> ) forms of <b>4</b> .....	13
7	Structures of <b>6a</b> and <b>6b</b> , and interaction between <b>6b</b> and active site of HMGCR.....	15
8	Structures of 5 compounds isolated and identified from chloroform fraction of <i>A. wilhelmsii</i> .....	16
9	Docking analysis of simvastatin and the QDF peptide with the HMG-CoA reductase.....	17
10	Mevalonate pathway of biosynthesis of cholesterol.....	18
11	Overview of Molecular Docking.....	24
12	Structure of designed BBR derivatives.....	35
13	The three-dimensional model of of HMGCR bound to <b>12</b> .....	36
14	The three-dimensional model of of PMK bound to <b>12</b> .....	37
15	Structure of compounds <b>11-15</b> and <b>35-44</b> .....	38

## LIST OF FIGURES (continued)

Figure		Page
16	Structure of designed BBR derivatives.....	40
17	HMGCR percentage inhibition values for BBR and its derivatives.....	44
18	Core structure of BBR derivatives ( <b>35-44</b> ).....	46
19	Structure of compound <b>41</b> and <b>42</b> .....	48
20	The binding interaction of compounds <b>41</b> (A) and <b>42</b> (B) with amino acids in active site of PMK.....	50
21	The binding interaction of compounds <b>41</b> (A) and <b>42</b> (B) with amino acids in active site of HMGCR.....	52
22	<sup>1</sup> H-NMR of compound <b>9</b> in CDCl <sub>3</sub> .....	59
23	<sup>1</sup> H-NMR of compound <b>10</b> in CDCl <sub>3</sub> .....	60
24	<sup>1</sup> H-NMR of compound <b>35</b> in CDCl <sub>3</sub> .....	61
25	<sup>1</sup> H-NMR of compound <b>36</b> in CDCl <sub>3</sub> .....	62
26	<sup>1</sup> H-NMR of compound <b>37</b> in CDCl <sub>3</sub> .....	63
27	<sup>1</sup> H-NMR of compound <b>38</b> in CDCl <sub>3</sub> .....	64
28	<sup>1</sup> H-NMR of compound <b>39</b> in CDCl <sub>3</sub> .....	65

# CHAPTER 1

## INTRODUCTION

### Background

Heart disease is the major health problem of people around the world. Drug developing heart disease treatment is a main focus of researchers. One known drug was statin, but the treatment may result in side effects such as myopathy, kidney failure, and liver function abnormalities. Thus, it is an urgent need to develop other drug candidates for eliminating these concerns. Hypercholesterolemia is an underlying factor leading to heart disease. By inhibiting the cholesterol synthesis pathway, scientists can develop ways to reduce the number of heart disease related deaths. There are several enzymes involved in the biosynthesis of cholesterol. HMG-CoA reductase (3-hydroxy-3-methyl-glutaryl-CoA reductase: HMGCR) is the key enzyme of cholesterol biosynthesis pathway in conversion of HMG-CoA to mevalonate. Phosphomevalonate kinase (PMK) catalyzes the next step reaction of phosphoryl transferred from adenosine triphosphate (ATP) to mevalonate-5-pyrophosphate (M5P) forming adenosine diphosphate (ADP) and melanonate 5-diphosphate with the aid of Magnesium ion ( $Mg^{2+}$ ). Thus the inhibition of the key enzyme HMGCR could lead to a decrease in cholesterol levels in the body. In case, however, the inhibition of HMGCR activity is incomplete, the metabolic pathway is not shut down. The sequential enzymes blocking of PMK in the next step should allow more effective cholesterol synthesis inhibition.

Berberine (BBR, 1, Figure 1) is a member of the protoberberine class of isoquinoline alkaloids, and has been reported to reduce low density lipoprotein cholesterol in animals and in hypercholestereolemic patients with almost none of side effects (Kong; et al. 2004: 1344-1351; Zhao; et al. 2008: 730-731; Kong; et al. 2008: 1029-1037). There was a previous study on the relationships between the structure and biological activity of berberine derivatives in order to determine the structural regions important for cholesterol-lowering activity. The structure activity relationship studies (SARs) showed that the methylenedioxy group on ring A, quaternary ammonium salt on ring C, and planar structure of berberine derivatives are essential for their up-regulatory activity on the low-density-lipoprotein receptor (LDLR) expression (Li; et al. 2009: 492-501). Substitution at C-8 of berberine with long aliphatic hydrocarbon chain ( $n = 10-20$ ) was more active in

cholesterol-lowering activity than that of Lovastatin drug (Ye; et al. 2012: 1353-1362). In this study, berberine derivatives will be designed and synthesized to evaluate the inhibition of HMGCR and PMK activities on the biosynthesis of cholesterol.

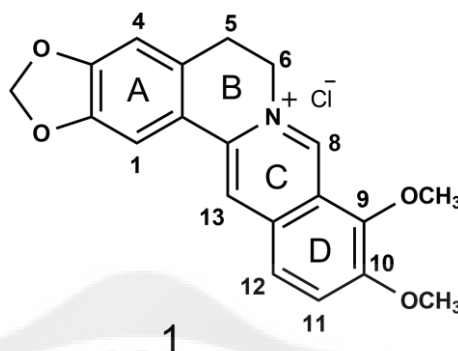


Figure 1 Structure of Berberine

### Molecular Docking

Molecular docking plays an important role in the rational design of drugs. In the field of molecular modeling, docking is a method which predicts the preferred orientation of one molecule to a second when bound to each other to form a stable complex. It can be defined as an optimization problem, which would describe the best fit orientation of a ligand that binds to a particular protein of interest. Molecular docking experiments were performed by using the scoring function or force field to obtain the free energy of binding. The intermolecular complex formed between protein with ligands and their binding modes of interaction had been tried to determine. In this module, the ligand was allowed to flexibility, whereas the protein was kept rigid and fixed during docking. Molecular docking was used as tools in this study to design berberine derivatives and predict the interaction between proteins, HMGCR and PMK, and berberine derivatives.

**Objectives of the research**

1. To design berberine derivatives using HMGCR- and PMK-based computer- aided drug design.
2. To study the interaction between berberine derivatives and proteins, HMGCR and PMK, using molecular docking.
3. To synthesize the designed berberine derivatives.
4. To evaluate the inhibition of HMGCR and PMK activities of the synthesized berberine derivatives.



## CHAPTER 2

### REVIEW OF LITERATURE

#### Cholesterol

Cholesterol is a steroid compound that has a unique structure and water insoluble property. The molecule is amphiphilic, having a hydrophobic hydrocarbon body and a hydrophilic hydroxyl headgroup. It is derived from food or synthesized in the body. Cholesterol has many important functions such as the composition of cell wall, source of bile and steroid hormones. Over the years, cholesterol has been considered as one of major health problems because it is a cause of cardiovascular disease. According to the World Health Organization, the leading cause of death worldwide is mainly from ischemic heart disease, coronary artery disease and cerebrovascular disease. All of these diseases are associated with high levels of cholesterol in blood (hypercholesterolemia or hyperlipidemia) (Cerqueira; et al. 2016: 5483-5506).

#### Biosynthesis of cholesterol

Biosynthesis pathway of cholesterol (Figure 2) occurs mostly in the membranes of endoplasmic reticulum (ER). The precursor is acetyl-coenzyme A (acetyl-CoA) which is derived from many species including glucose metabolites, fatty acid or amino acid with NADPH as coenzyme and ATP as energy. In the first step, mevalonate is synthesized from condensation of acetyl-CoA to acetoacetyl CoA then acetoacetyl CoA reacts with acetyl-CoA to give 3-hydroxy-3-methyl-glutaryl-CoA (HMG-CoA). Subsequently, HMG-CoA is converted to mevalonate catalyzed by 3-hydroxy-3-methyl-glutaryl-CoA reductase (HMGCR). This step is not only the committed step of the whole process but also the rate-limiting one. In the second step, the mevalonate (6C) is phosphorylated to form 3-phospho-5-pyrophosphomevalonate catalyzed by phosphomevalonate kinase (PMK). The phosphate groups are donated by 3 molecules of ATP. Then the activated isoprene unit,  $\Delta^3$ -isopentenyl pyrophosphate, is achieved by releasing carbon dioxide from 3-phospho-5-pyrophosphomevalonate. Subsequently isomerization of  $\Delta^3$ -isopentenyl pyrophosphate gives dimethylallyl pyrophosphate. In the last step, a series of successive condensations of

activated isoprenes, a 30-carbon linear structure of squalene is formed. Squalene is the biochemical precursor of all steroids, which undergoes cyclization to give lanosterol and then transformed to cholesterol by removing of three carbons from lanosterol (Cerqueira; et al. 2016: 5483-5506).



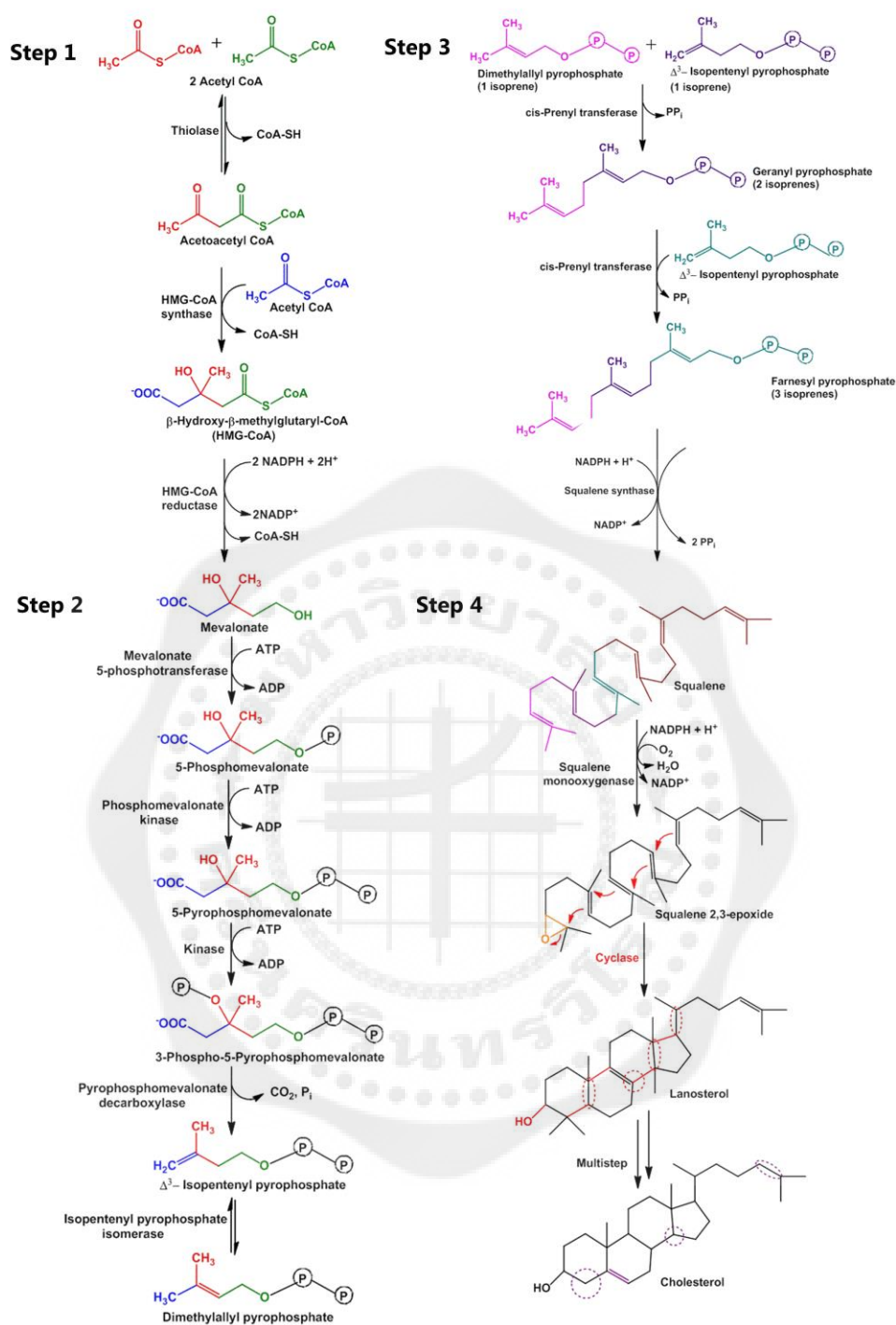


Figure 2 Biosynthesis of cholesterol.

Modified from Cerqueira, N. M. F. S. A., Oliveira, E. F., Gesto, D. S., Diogo Santos-Martins., Moreira C., Moorthy, H. N., Ramos, M. J., Fernandes, P. A. Cholesterol biosynthesis: a mechanistic overview *Biochemistry*. 2016, 55, 5483-5506.

## **Berberine**

Berberine (BBR, 1), an isoquinoline alkaloid extracted from Chinese, Thai, and American medicinal plants, is a major component of many plants such as *Rhizoma coptidis*, *Berberis vulgaris* (barberry), *Berberis aristata* (tree turmeric), *Mahonia aquifolium* (Oregon grape), *Hydrastis canadensis* (goldenseal), *Xanthorhiza simplicissima* (yellowroot), *Phellodendron amurense* (Amur cork tree), *Coptis chinensis* (Chinese goldthread), *Tinospora cordifolia*, *Argemone mexicana* (prickly poppy), and *Eschscholzia californica* (Californian poppy). BBR has various biological activities such as anticancer (Pandey; et al. 2008: 5370-5379), antihyperglycemia (Tang; et al. 2006: 109-115), antihyperlipidemia (Cicero; et al. 2007: 26-30), and anti-heart failure functions (Zeng; et al. 2003: 173-176). BBR has been reported to reduce serum low density lipoprotein cholesterol, which was mediated by increasing LDLR expression at the post-transcriptional level through stabilization of LDLR messenger RNA (LDLR mRNA) in an extracellular signal-regulated kinase-dependent manner, a mechanism distinct from that of cholesterol-lowering Statin drugs (Kong; et al. 2004: 1344-1351).

## **Biological activities of Berberine and berberine derivatives**

In 2004, Kong et al. identified that BBR was a novel cholesterol lowering drug working through a unique mechanism distinct from statin by up-regulating LDLR expression at transcriptional level. The LDL receptor is only receptor capable of clearing significant amounts of LDL from plasma. Among a variety of herb samples in Chinese medicines, BBR showed the highest activity with a 3.5-fold increase in LDLR mRNA and a 2.6-fold increase in LDLR protein in the liver of hamsters treated with BBR 100 mg/kg. Moreover it reduced serum cholesterol by 29%, triglycerides (TGs) by 35% and LDL-cholesterol (LDL-c) by 25% when 32 hypercholesterol patients were given 500 mg of BBR orally twice per day for 3 months. In animal study, they were conducted in hamsters which fed a high-fat and high-cholesterol (HFHC) diet for 2 weeks. Treatment with BBR (100 mg/kg/day) by oral administration for 10 days allowed helping lower LDL-c by 42% compared to statin drug (Kong; et al. 2004: 1344-1351).

In 2006, Brusq et al. identified an additional mechanism for the hypolipidemic effects of BBR. Treatment of hyperlipidemic hamsters with BBR decreased plasma LDL-c

and reduced fat storage in the liver. The results revealed that BBR not only up-regulates the LDLR expression but also inhibits lipid synthesis in human hepatocytes by activated the AMPK. These effects could explain the strong reduction of plasma TGs observed with BBR in clinical trials (Brusq; et al. 2006: 1281-1288).

In 2008, Kong et al. combined BBR with statins to enhance lipid-lowering effect, reduced dosage of statins and decreased risk of side effects. The results showed that the combination of BBR with simvastatin (SIMVA) increased the LDLR gene expression higher than the use of BBR or simvastatin alone. In the treatment of food-induced hyperlipidemic rats, the combination therapy of BBR (90 mg/kg/day, oral) with SIMVA (6 mg/kg/d, oral) reduced serum LDL cholesterol by 46.2%, which was more effective than that of the SIMVA monotherapy at 6 mg/kg/d (28.3%) or BBR at 90 mg/kg/d (26.8%) and similar to that of SIMVA at 12 mg/kg/day (43.4%). More effective reduction of serum triglyceride was also achieved with the combination therapy as compared with either monotherapy. The combination of BBR with SIMVA up-regulated the LDLR mRNA in rat livers to a level about 1.6-fold higher than the monotherapy did. Significant reduction of liver fat storage and improved liver histology were found after the combination therapy. The therapeutic efficacy of the combination was then evaluated in 63 hypercholesterolemic patients. As compared with monotherapy, the combination showed an improved lipid-lowering effect with 31.8% reduction of serum LDL-c (Kong; et al. 2008: 1029-1037).

In 2011, Marazzi et al. studies on the effect of nutraceuticals (containing BBR 500 mg, policosanol 10 mg, red yeast rice 200 mg, folic acid 0.2 mg, coenzyme Q10 2.0 mg, and astaxanthin 0.5 mg) on 40 patients that had high total cholesterolemia, high LDL-c, and were older than 75 years of age for 3, 6, and 12 months. The results show that they could significantly reduce total cholesterolemia (20%), LDL-c (31%), and insulin resistance (10%) and no one died or injured during the study. Combined nutraceuticals was also safe and well tolerated in these patients (Marazzi; et al. 2011: 1105–1113).

In 2012, Xiao et al. studied the effect of BBR on PCSK9-LDLR pathway in C57BL/6 mice with lipopolysaccharide (LPS) induced inflammation. The combination of LPS with berberine was investigated including 5 mg/kg LPS plus 10 mg/kg BBR, and 5 mg/kg LPS plus 30 mg/kg berberine. The results showed that both concentrations of BBR (10 and 30 mg/kg) increased hepatic mRNA and protein expressions of LDLR in mice ( $p < 0.05$  or  $p$

< 0.01). Furthermore BBR (10 and 30 mg/kg) increased plasma HDL-c level and decreased plasma LDL-c, TG and total cholesterol (TC) concentrations compared with control group (Xiao; et al. 2012: 889-895).

In the same year, Ye et al. designed and synthesized 8-alkyl berberine derivatives with a long aliphatic chain ( $n = 10-20$ ) to evaluate their antihyperlipidemic activity. (Figure 3) The inhibition against HMGCR activity in vitro and the antihyperlipidemic effect in vivo of 8-alkyl berberine derivatives revealed that the introduction of an alkyl group at C-8 increased the activities as the alkyl side chain length increased. Especially, 8-hexadecyl berberine (**2D**) showed the highest activity (Table 1.), which was better than that of lovastatin drug. The interaction between HMGR receptor and berberine derivative ligand resulting from molecular docking study indicated that the highest antihyperlipidemic efficacy of **2D** was exerted by a dual mechanism of inhibiting HMGR activity like statin and lowering the level of low density lipoprotein-cholesterol like berberine (Ye; et al. 2012: 1353-1362).

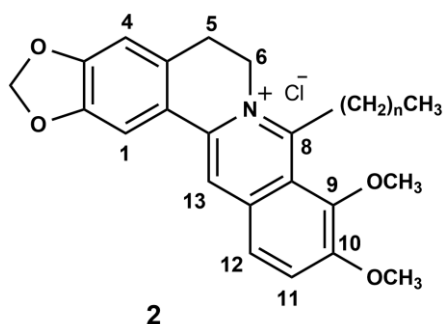


Figure 3 Structure of 8-alkyl berberine derivatives. n is number of methylene group.

(Ye; et al. 2012: 1353-1362).

Table 1. Inhibitory rate of 8-alkyl-berberine against HMGR and their LD<sub>50</sub> (Ye; et al. 2012: 1353-1362).

Compound	C (μmol/l)	Inhibitory rate (%)	LD <sub>50</sub> (mg/kg)
Lovastatin	8.0	20.2 ± 1.4	> 1000
Berberine (1)	8.0	Not be detected	763.5
8-Octyl-berberine (2A)	8.0	Not be detected	534
8-Dodecyl-berberine (2B)	8.0	4.2 ± 0.9	752
8-Tetradecyl-berberine (2C)	8.0	11.2 ± 0.5	803
8-Hexadecyl-berberine (2D)	8.0	42.7 ± 2.7	> 1000
8-Octadecyl-berberine (2E)	8.0	33.0 ± 1.8	> 1000

In 2017, Hao et al. designed and synthesized a hybrid compound of berberine and baicelin, call as BBS (Figure 4), which were evaluated in 3T3-L1 adipocytes, the adipocyte morphology increased the synthesis and accumulation of triglycerides. The results indicated that BBS show the greatest effect on against 3T3-L1 cells than baicalein, and berberine with  $IC_{50}$  values of  $9.42 \pm 0.60$ ,  $29.81 \pm 0.90$  and  $21.84 \pm 1.67$  mM, respectively (Hao; et al. 2017: 5506–5512).

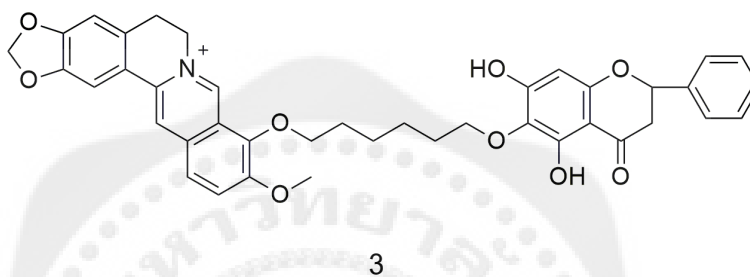


Figure 4 Structure of berberine-baicalein (BBS).

### 3-Hydroxy-3-methyl-glutaryl-CoA reductase

HMG-CoA reductase (3-hydroxy-3-methyl-glutaryl-CoA reductase: HMGR) is the key enzyme of cholesterol biosynthesis pathway in conversion of HMG-CoA to mevalonate. Hence HMGR could be the target enzyme to decrease cholesterol levels.

In 1976, Endo et al. isolated three metabolites, **4A**, **4B** and **4C** produced from *Penicillium citrinum*, and evaluated inhibitory effect on  $^{14}\text{C}$ -acetate conversion into digonin precipitable sterols in a rat liver enzyme system. Compound **4B** showed the highest inhibitory effect and cholesterol synthesis reduction to 50% of control at the concentration of  $0.026\ \mu\text{M}$ . In normal rats, the single oral administration of the three metabolites at dose of 5 and 20 mg/kg could reduce serum cholesterol at 3 hours after their administration. **4B** could help to lower the levels of serum cholesterol by approximately 30 % at a dose of 20 mg/kg. These studies led to the discovery of a potent HMG-CoA reductase inhibitor, named mevastatin (formerly called **4B** or compactin) (Endo; et al. 1976A: 1346-1348).

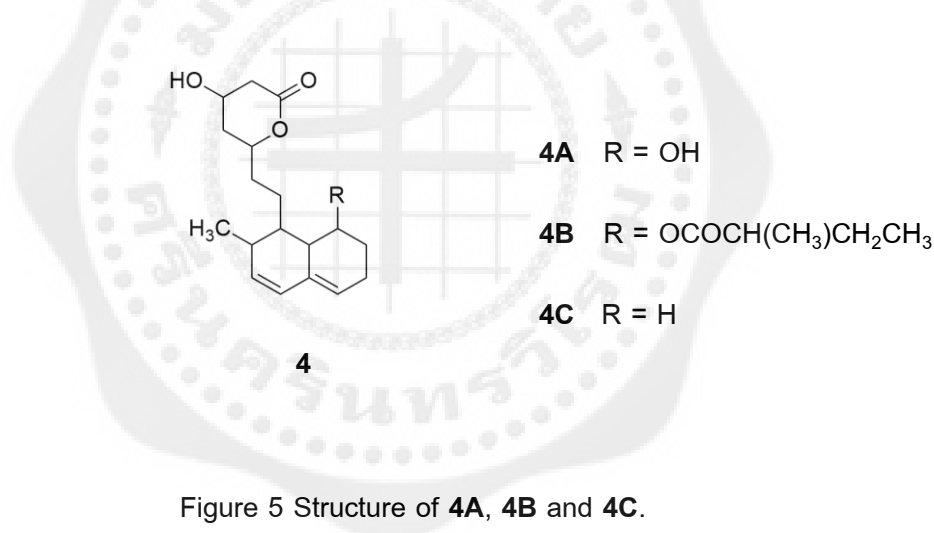
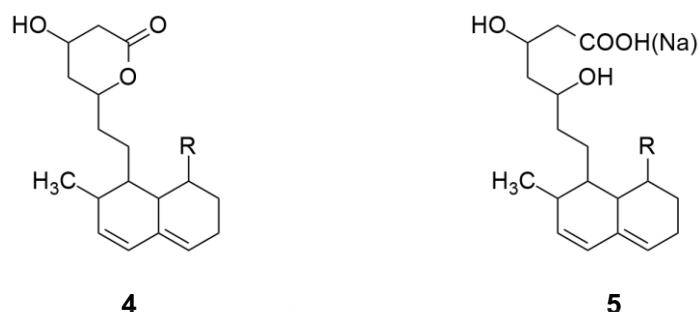


Figure 5 Structure of **4A**, **4B** and **4C**.

In 1976, the same research group indicated that mevastatin has a hexahydronaphthalene skeleton substituted with a  $\beta$ -hydroxy- $\delta$ -lactone moiety, which can be converted into the water-soluble open chain acid or carboxylate salt by treatment with alkali (Figure 6). Interestingly, lactone and acid forms of **4B** were shown to inhibit sterol syntheses from both  $[^{14}\text{C}]$  acetate with  $\text{IC}_{50} = 0.026\ \mu\text{M}$  and  $0.014\ \mu\text{M}$ , and  $[^{14}\text{C}]$  HMG-CoA with  $\text{IC}_{50} = 0.1\ \mu\text{M}$  and  $0.023\ \mu\text{M}$ , respectively, but showed no effect on the conversion of  $[^3\text{H}]$  mevalonate into sterols. The results demonstrated mevastatin to be a potent inhibitor for HMG-CoA reductase. Subsequently, the search for additional HMG-CoA reductase

inhibitors was continued for many years, leading to the isolation of several compounds of the mevastatin family. (Endo; et al. 1976B)



**4A** R = -OH

**4B** R = -OCOCH(CH<sub>3</sub>)CH<sub>2</sub>CH<sub>3</sub>

Figure 6 Lactone (**4**) and acid (**5**) forms of **4** (Endo; et al. 1976B: 323-326).

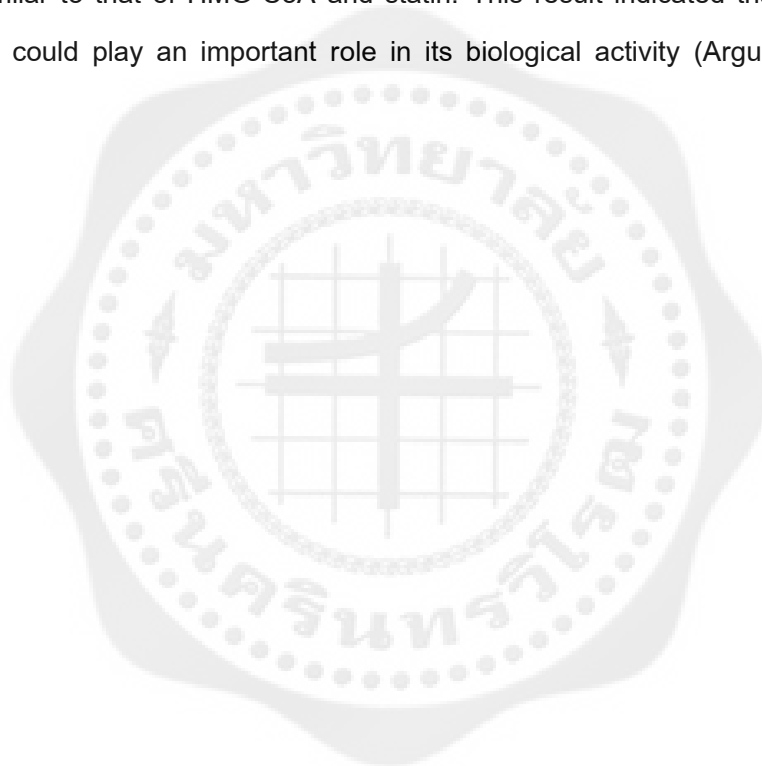
In 2015, Mijares et al. investigated the effect of simvastatin and ezetimibe on mitochondrial function and leukocyte endothelium interactions in polymorphonuclear cells of hyperlipidemic patients. Treatment of 39 hyperlipidemic patients with either simvastatin or ezetimibe decreased LDLc by 40.2% and 19.6%, respectively, and increased non-HDLc by 37.1% and 18.8%, respectively. The combination of 40 mg/day simvastatin with 10 mg/day ezetimibe for 4 weeks reduced LDLc by 50.7-56.8%, and increased non-HDLc level by 46.0-52.9% (Mijares; et al. 2015: 40-47).

Nowadays, statin has been widely used to decrease lipid in blood by blocking HMGCR in the mevalonate pathway of cholesterol biosynthesis. Meanwhile it has many side effects such as myopathy, kidney failure, and liver function abnormalities. Therefore, it is necessary to find new drugs that can decrease cholesterol levels in the body (Bitzur; et al. 2013: 2).

In 2009, Singh et al. evaluated the effect of green and black tea on cholesterol synthesis. The results showed that black tea extract 100 µg/mL reduced cholesterol synthesis by 78% while green tea extract 250 µg/mL reduced by 55%. Then black and green teas were evaluated for the effect on HMG-CoA reductase activity. The results showed that black tea and green tea extract at 100 µg/mL decreased HMG-CoA reductase

activity by 43 and 34%, respectively. These findings indicated that green and black teas contain compounds capable of directly inhibiting HMG-CoA reductase (Singh; et al. 2009: 816-822).

In 2010, Arguelles et al. designed a series of  $\alpha$ -asarone by using molecular docking and evaluated their hypolipidemic activity in a murine model. It showed the highly hypocholesterolemic activity corresponding to the docking results. Among the most active analogues, **6a** and **6b** had the lowest binding energy due to hydrogen bond interactions between the carboxylic group and the polar side-chains of Ser684, Lys692 and Lys735 (Figure 7) similar to that of HMG-CoA and statin. This result indicated that the polar group of compound could play an important role in its biological activity (Arguelles; et al. 2012: 4238-4248).



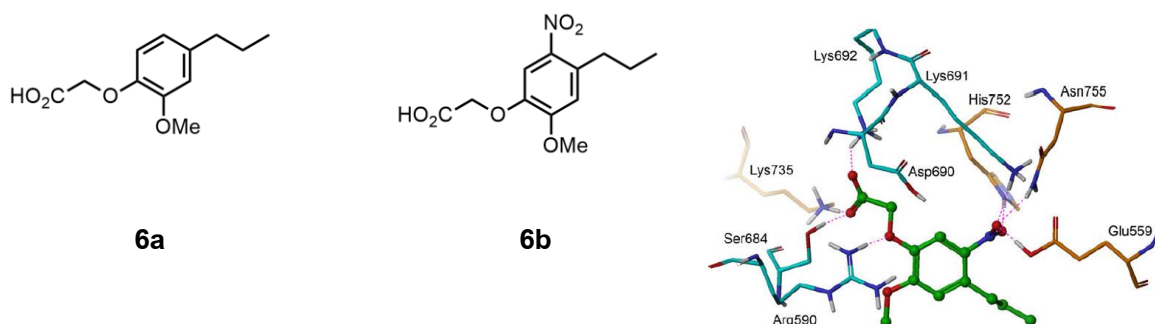


Figure 7 Structures of **6a** and **6b**, and interaction between **6b** and active site of HMGCR.

Modified from Argelles, N., Sanchez-Sandoval, E., Mendieta, A., Villa-Tanaca, L., Garduno-Siciliano, L., Jimenez, F., Cruz, M. d. C., Medina-Franco, J. L., Chamorro-Cevallos, G., Tamariz, J. Design, synthesis, and docking of highly hypolipidemic agents: *Schizosaccharomyces pombe* as a new model for evaluating  $\alpha$ -asarone-based HMG-CoA reductase inhibitors. *Bioorganic & Medicinal Chemistry*. **2010**, 18, 4238–4248.

In 2010, Wei et al. screened HMGCR inhibitors from composite *Salvia Miltiorrhiza* (CSM) by molecular docking, evaluated the performance of method to confirm the obtained results. They compared the predicted  $IC_{50}$  with experiment  $IC_{50}$  of ten HMGCR inhibitors from MDL Drug Data Report (MDDR). The correlation coefficient ( $R^2$ ) between  $-\Delta G$  and  $-\text{Log}(IC_{50})$  was 0.865. Four phenolic compounds in CSM collection showed potential inhibition of HMGCR with binding free energy value of  $-9$  kcal/mol ( $IC_{50} < 10$  nmol/L) (Wei; et al. 2010: 0051-0056).

In 2016, Khazneh et al. identified the compounds obtained from *Achillea wilhelmsii* to evaluate their hypoglycemic and anti-hypercholesterolemic activities, and effect on inflammatory mediators. The anti-hypercholesterolemic activity was evaluated in vitro using the 3-hydroxy-3-methylglutaryl-CoA (HMG-CoA) reductase assay kit. The chloroform fraction (CF) showed the most significant 3-hydroxy-3-methylglutaryl-CoA reductase (HMGR) inhibition activity. Five main compounds in the CF were isolated and identified. There were only two compounds, 1,10-epoxydesacetoxymatricarin (CP1) and leucodin (CP2), found to be active against hypercholesterolemic with  $IC_{50}$  values of  $6.37$   $\mu\text{M}$  and  $3.88$   $\mu\text{M}$ , respectively (Khazneh; et al. 2016: 404).

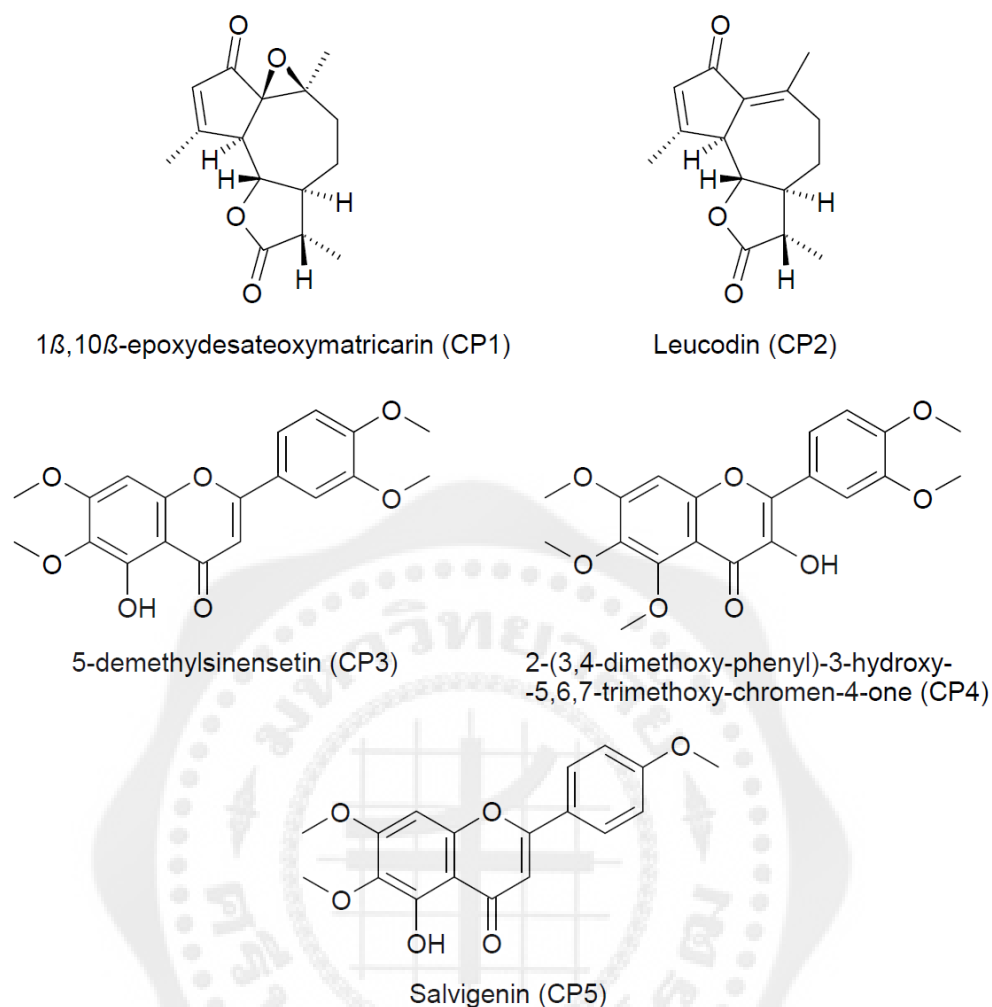


Figure 8 Structures of 5 compounds isolated and identified from chloroform fraction of *A. wilhelmsii*.

Modified from Khazneh, E., Hribova, P., Hosek, J., Suchy, P., Kollar, P., Prazanova, G., Muselik, J., Hanakova, Z., Vaclavik, J., Milek, M., Legath, J., Smejkal, K. The chemical composition of *Achillea wilhelmsii* C. Koch and its desirable effects on hyperglycemia, inflammatory mediators and hypercholesterolemia as risk factors for cardiometabolic disease. *Molecules*. **2016**, 21, 404.

In 2018, Silva et al. evaluated the biological activity of the fraction containing peptides of < 3 kDa, as well as that of the Gln-Asp-Phe (QDF) peptide, derived from cowpea  $\beta$ -vignin protein, to inhibit HMG-CoA reductase activity. In vitro study, the results

showed that the tripeptide QDF inhibits HMG-CoA reductase with  $IC_{50}$  values of 12.8  $\mu$ M. And in silico study, the QDF peptide showed binding interaction with amino acid residues in active site of HMG-CoA reductase such as Lys692, Arg590, Ser589, Ser565 similar to simvastatin as shown in Figure 9.

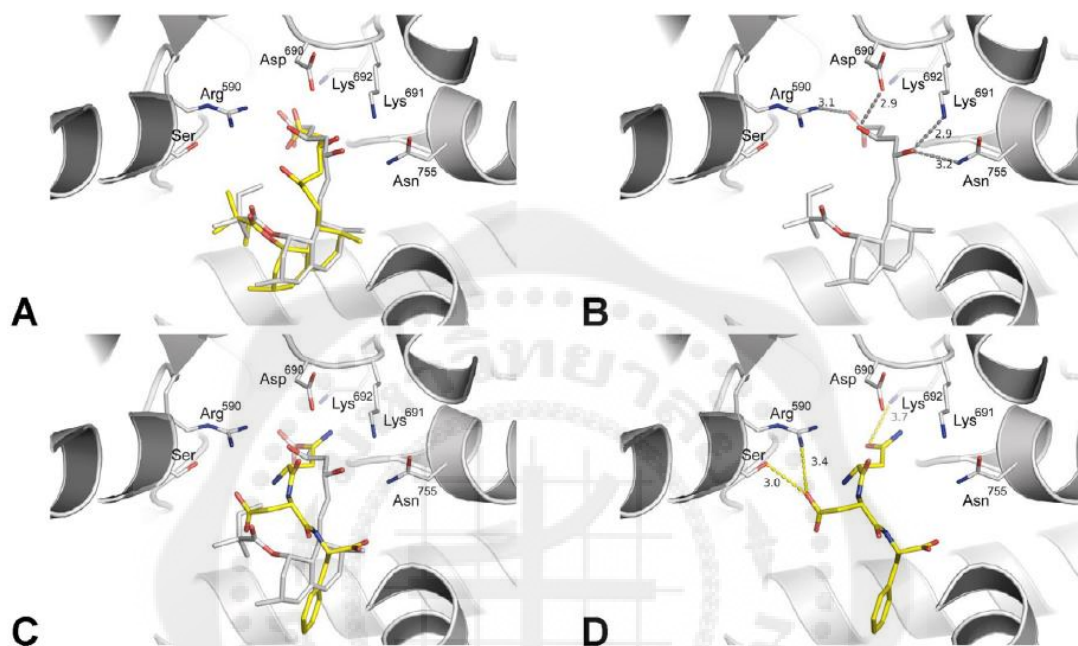


Figure 9 Docking analysis of simvastatin and the QDF peptide with the HMG-CoA reductase catalytic complex (PDB ID: 1HW9) using the AutoDock-VINA software. Best-ranked pose for simvastatin (yellow) and the binding profile of crystallographic simvastatin (grey) in the HMGCoA-reductase active site (B). Orientation of the QDF peptide docked into HMGCoA-reductase active site in comparison to the bioactive simvastatin conformation (C) and its predicted binding profile in the active site (D).

Modified from Silvaa, M. B. C., Souzaa, C. A. C., Philadelpha, B. O., Cunhaa, M. M. N., Batistaa, F. P. R., Silvaa, J. R., Druziana, J. L., Castilhoa, M. S., Cillib, E. M., Ferreira, E. S. In vitro and in silico studies of 3-hydroxy-3-methyl-glutaryl coenzyme A reductase inhibitory activity of the cowpea Gln-Asp-Phe peptide. *Food Chemistry*. **2018**, 259, 270–277.

### Phosphomevalonate Kinase (PMK)

Phosphomevalonate kinase (PMK, EC2.7.4.2) catalyzes the rate-limiting step in isoprenoid/sterol biosynthesis, providing a variety of products that are necessary for growth of mammalian cells such as cholesterol, bile acids, heme A, dolichol, and ubiquinone (Doun et al., 2005; Eyzaguirre et al., 2006). PMK is in the mevalonate biosynthetic pathway, downstream of HMG CoA reductase as shown in Figure 10.

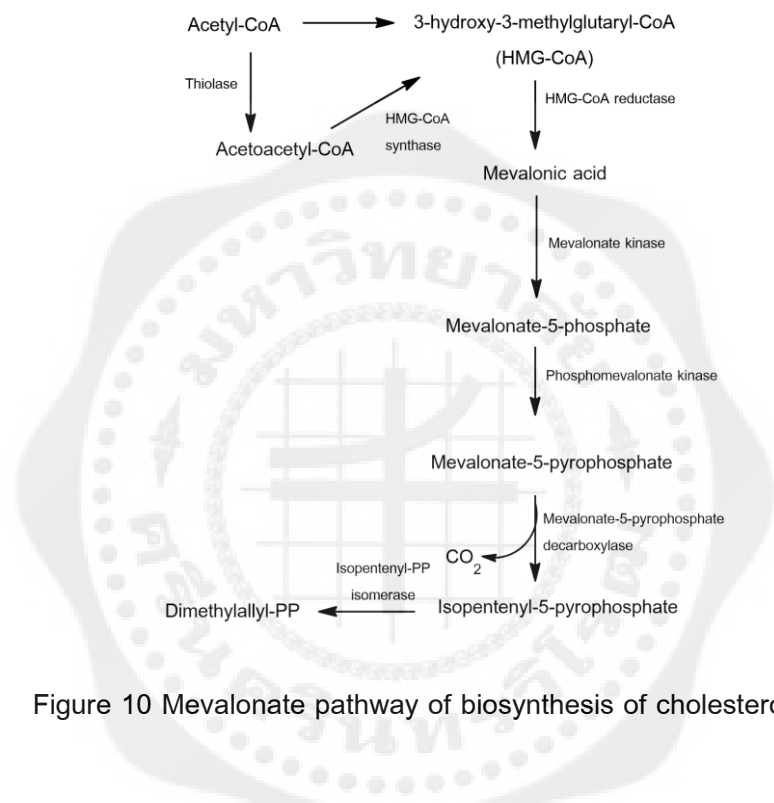


Figure 10 Mevalonate pathway of biosynthesis of cholesterol.

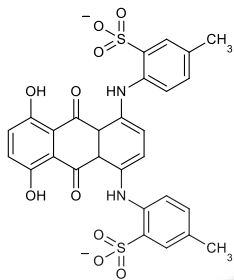
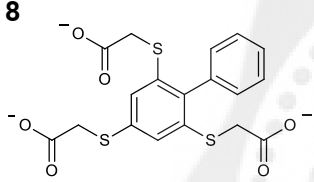
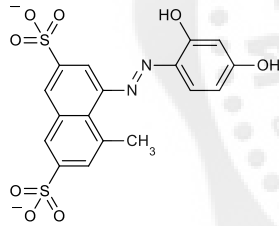
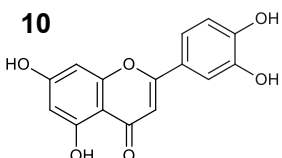
Modified from Buhaescu, I., Izzedine, H. Mevalonate pathway: A review of clinical and therapeutical implication. *Clinical Biochemistry*. 2007, 40, 575-584.

Based on structural investigations and mechanisms, PMK consists of two domains. The larger ATP-binding domain is composed of a five stranded parallel  $\beta$ -sheet interweaved with three  $\alpha$ -helices. The smaller M5P domain is composed of loop regions and two  $\alpha$ -helices. This enzyme has a catalytic activities of phosphoryl transferring as to convert mevalonate 5-phosphate (M5P) and adenosine-5'-triphosphate (ATP) to mevalonate 5-diphosphate and adenosine diphosphate (ADP) (Bazaes; et al. 1980: 2305-2310; Bloch; et al. 1959: 2595–2604; Ferrand; et al. 2011: 637–646; Herdendorf and Miziorko; 2006: 3235–3242; Miziorko; 2011: 131–143).

However, some aspect of the mechanism of this protein in catalysis reactions remains unclear. Herdendorf and Miziorko investigated the functional evaluation of conserved basic residues in human PMK and suggested that R110 was important for human PMK catalysis (Herdendorf and Miziorko; 2007: 11780-11788). However, R111 and R84 were situated close to the “Walker B” motif that occurred the phosphate transfer reaction between acceptor and donor atoms in the molecule. At the C-terminal end of the adjacent  $\beta$  strand 3 are four hydrophobic residues followed by invariant S107 and D108. Properties of these polar side chains and proximity to a putative ATP binding loop suggested that this region represents a “walker B” motif usually associated with the binding of the cation of MgATP (Koonin; 1993: 1165–1174; Leipe; et al. 2003: 781–815).

In 2013, Boonsri et al. screened novel PMK inhibitors using autodock and measured their affinities using NMR and fluorescence titration. The results obtained, among 26 compounds were screened with NMR experiments, four compounds **7-10** exhibit potential affinity for PMK (Table 2.). Then fluorescence titrations were conducted to confirm their binding affinity to PMK. It was found that docking yielded a hit rate of 15% and identified reasonably potent PMK inhibitors with  $K_d$  values in the range of 6 – 60  $\mu$ M (Boonsri; et al. 2013: 313-319).

Table 2. Structures of potential PMK inhibitors 7-10.

Inhibitor	Predicted lowest binding energy (kcal/mol)	$K_d$ ( $\mu$ M) NMR [residue used for data fitting]	$K_d$ ( $\mu$ M) fluorescence
<b>7</b> 	-11.6	$55.4 \pm 12.9$ [G177]	$31 \pm 8$
<b>8</b> 	-10.34	$6.3 \pm 5.7$ [T128]	$14.6 \pm 4.6$
<b>9</b> 	-11.8	ND <sup>a</sup> [Q136]	$12 \pm 2$
<b>10</b> 	-9.2	ND <sup>a</sup> [A172]	$61.0 \pm 19.5$

<sup>a</sup> The NMR fit was not reliable because in addition to a specific binding event that seems to occur at low concentrations, there is also a non-specific effect that does not plateau.

Modified from Boonsri, P., Neumann, T. S., Olson, A. L., Cai, S., Herdendorf, T. J., Miziorko, H. M., Hannongbua, S., Sem, D. S. Molecular docking and NMR binding studies to identify novel inhibitors of human phosphomevalonate kinase. *Biochem. Biophys. Res. Commun.* **2013**, 430, 313–319.

## CHAPTER 3

### EXPERIMENTAL

#### General Instrument

Autopipette  
Bruker 300 MHz NMR spectroscopy  
Centrifuge  
Heat Box  
pH meter  
UV Spectrophotometer  
SpectraMax M2 microplate readers  
Sealed tube

#### Chemical

Acrylamide (Bio Basic, Canada)  
Agar bacteriologico americano (Pronadisa, Spain)  
Ampicillin (Sigma, USA)  
Bis-acrylamide (Bio Basic, Canada)  
Coomassie brilliant blue R-250 (Bio Basic, Canada)  
Dimethyl sulfoxide (DMSO) (Labscan, Thailand)  
Glycerol (99%, Ajax Finechem, Australia)  
Sodium dodecyl sulfate (SDS) (Bio Basic, USA)  
Tetramethylethylenediamine (TEMED) (Bio Basic, USA)  
Tris (hydroxymethyl) aminomethane (Research Organic, USA)  
Tryptone type-I (Himedia, India)  
Yeast extract powder (Himedia, India)  
Berberine (chloride salt) ( $\geq 90\%$ , Sigma Aldrich)  
Sodium hydroxide (97 %, Carlo Erba)

Acetonitrile (AR grade, ACI Labscan)  
1-(chloromethyl)naphthalene (90 %, Sigma Aldrich)  
Dimethyl formamide (99.5 %, Merck)  
Silica gel (SiliCycle, SILSAFLASH G60, 230-400 mesh)  
Aluminium oxide 90 active neutral (E. Merck, 70-230 mesh)  
*tert*-butyl bromoacetate (98 %, Sigma Aldrich)  
*tert*-butyl 3-bromopropionate (98 %, Sigma Aldrich)  
Trifluoroacetic acid (99%, extra pure, Acros organics)  
Methyl 4-bromobutyrate (> 98.0 %, Tokyo Chemical Industry co., ltd.)  
Methyl 5-bromovalerate (> 97.0 %, Tokyo Chemical Industry co., ltd.)  
Ethyl 6-bromohexanoate (> 98.0 %, Tokyo Chemical Industry co., ltd.)  
Deuteriochloroform (CDCl<sub>3</sub>) (99.8%, Cambridge Isotope Laboratories, Inc)  
Deuteriomethanol (CD<sub>3</sub>OD) (99.8%, Cambridge Isotope Laboratories, Inc)  
TLC plates (20 x 20, 0.5 mm thick, E. Merck)  
Human Phosphomevalonate kinase (PMK) pET15b expression plasmid from  
Henry Miziorko (Addgene plasmid # 52430).  
HMGR assay kit from Sigma-Aldrich, Catalog Number CS1090  
Potassium carbonate (98-100%, Riedel-de Haën)

## Method

### 1. Molecular docking of PMK

The stable 3D structure of the berberine and its derivatives called as ligand was energy minimized at the HF/6-31G by using G09 program. Discovery Studio 4.0 was used to convert to chemical files to mol2 format (Molecular Networks).

The structure of PMK protein (PDB code 3CH4) was obtained from PDB [Research Collaboratory for Structural Bioinformatics (RCSB), (<https://www.rcsb.org/pdb>)]. The binding orientation of ligands in this PMK (human) was determined using Autodock 4.0. Gasteiger charges and hydrogens were added using Autodock Tools (ADT). The docking grids were also prepared using ADT with a grid box created with 60 x 60 x 60 points and a resolution of

0.375 Å. After the grid box was centered in the ligand, grid potential maps were calculated using module AutoGrid 4.0.

The protein pdb files and grid maps were all prepared using the AutoDock Tools suite (Morris et al., 2009). Grid maps are used in the energy calculations performed by Autodock. The protein was tested just as the ligands were (done manually on AutoDock Tools), adding partial charges and merging all non-polar hydrogens and saved as pdbqt file. All 13 different grid maps available in AutoDock were generated using AutoGrid4 with grid box, the site used to dock the ligands, placed over the active sites of the protein.

The docking parameter file (dpf), which contains the parameters that AutoDock uses to dock the ligand into the protein, was prepared using ADT, and default docking parameters were used by using genetic algorithm approach (ga), except that 150 ga runs were used with 2,500,000 as the maximum number of evaluations and a root mean square deviation (RMSD) tolerance set to 2.0 angstroms. The docking results were then clustered on the basis of the RMSD between the coordinates of the atoms in a given ligand, and were ranked on the basis of calculated free energy of binding. The docking log files were then analyzed which rank orders all the dockings by binding energy. The results were then analyzed to find the best clustered compounds with lowest free energy of binding.

## **2. Molecular docking of HMGCR**

Molecular docking study of HMGCR (PDB code 3DCB ) were performed similarly to PMK protein excluding the grid box was changed to 60 x 60 x 52 points.

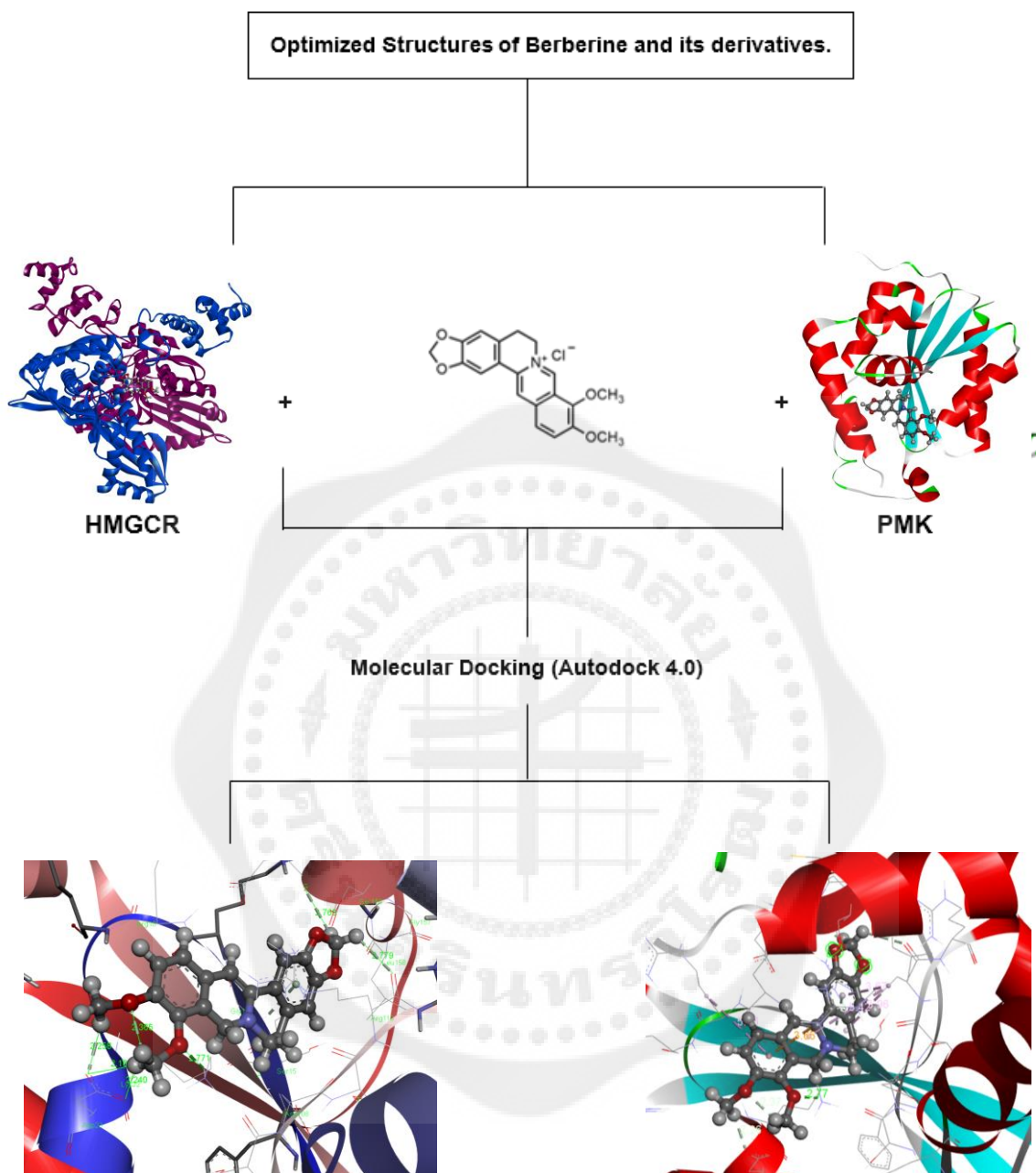


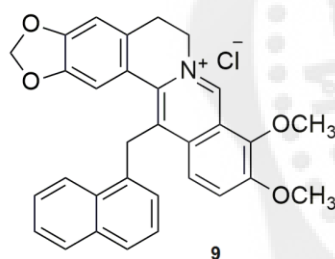
Figure 11 Overview of Molecular Docking.

### 3. Synthesis

Berberine chloride and reagents were obtained from the Sigma-Aldrich Chemicals company. Solvents were purified and dried by standard techniques. (Perrin, D. D.; Armarego, W. L. F. Purification of Laboratory Chemicals; 3rd ed.; Pergamon Press Ltd.: Oxford, 1988.) Column Chromatography was performed using Merck Kieselgel 60 silica gel (230-400 mesh) or Aluminium oxide 90 active neutral (70-230 mesh). All chromatographic solvent proportions are volume for volume. Reactions were monitored by thin-layer chromatography (TLC) on Merck silica gel 60 F254 and the compounds were detected by examination under ultraviolet light.

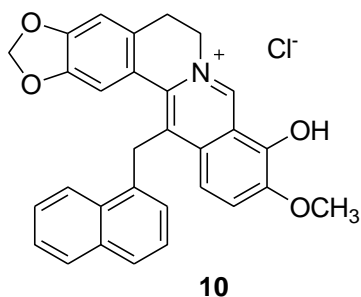
The  $^1\text{H}$  NMR was determined at 299.92 MHz with a Bruker-300 spectrometer. The spectra were obtained from solutions in  $\text{CDCl}_3$  or  $\text{CDCl}_3/\text{CD}_3\text{OD}$ . High resolution electrospray ionization mass spectra, ESI-MS, were obtained with a Thermo Finnigan LC-Q mass spectrometer.

#### 3.1 Synthesis of 13-(1-naphthalenylmethyl)berberine (9)



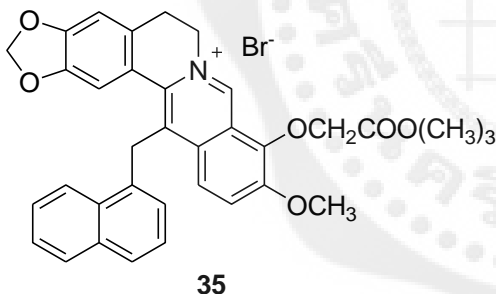
To a suspension of berberine (1) (1.0 g, 2.97mmol) in acetone (30 mL), was added 30% aqueous sodium hydroxide (35 mL). The mixture was heated at 65°C for 30 min. The reaction mixture was concentrated and then poured into ice water (200 mL). The precipitate was filtered and dried to give 8-acetyl dihydroberberine (8) (0.989 g, 2.61 mmol) as a pale yellow solid which was then dissolved in acetonitrile (30 mL) and add 1-(chloromethyl)naphthalene (1 mL, 6.68 mmol). The reaction was refluxed at 80 °C for 6h. The mixture was concentrated and chromatographed on neutral alumina (2 % MeOH in DCM) to give 13-(1-naphthalenylmethyl) berberine (9) (245 mg, 21%) as a yellow solid.  $^1\text{H}$  NMR ( $\text{CD}_3\text{OD}/\text{CDCl}_3$ ):  $\delta$  10.79 (s, 1H, 8-H), 7.56 (d, 2H, J = 9.37 Hz, 11-H), 7.42 (d, 2H, J = 9.34 Hz, 12-H), 7.64 (s, 1H, 1-H), 7.2-8.1 (m, 7H, naphthyl Ar-H), 5.90 (s, 2H,  $\text{OCH}_2\text{O}$ ), 5.35 (br s, 2H, 6-H), 4.97 (s, 2H,  $\text{CH}_2\text{-Ph}$ ), 3.20 (br s, 2H, 5-H), 4.30 (s, 3H, 9- $\text{OCH}_3$ ), 4.0 (s, 3H, 10- $\text{OCH}_3$ ). HRMS (ESI): m/z calcd for  $\text{C}_{31}\text{H}_{26}\text{NO}_4$   $[\text{M}]^+$  : 476.1827; found: 476.1856.

### 3.2 Synthesis of 13-(1-naphthalenylmethyl)berberubine (**10**)

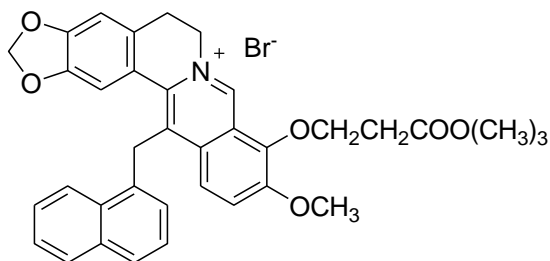


A yellow suspension of 13-(1-naphthalenylmethyl)berberine (**9**) (0.25 g, 0.52 mmol) in dimethyl formamide (DMF, 1 mL) in a sealed tube was heated at 150 °C for 2h. The resulting red solution was cooled to room temperature and then concentrated. The residue was concentrated and chromatographed on neutral alumina (1 % MeOH in DCM) to give 13-(1-naphthalenylmethyl)berberubine (**10**) (100 mg, 0.22 mmol, 42 %) as a red solid.  $^1\text{H}$  NMR ( $\text{CD}_3\text{OD}/\text{CDCl}_3$ ):  $\delta$  9.45 (s, 1H, 8-H), 6.86 (s, 1H, 4-H), 6.75 (s, 1H, 1-H), 7.2-8.1 (m, 7H, naphthyl Ar-H), 5.81 (s, 2H,  $\text{OCH}_2\text{O}$ ), 4.43 (br s, 2H, 6-H), 4.76 (s, 2H,  $\text{CH}_2\text{-Ph}$ ), 3.03 (br s, 2H, 5-H), 3.80 (s, 3H, 10- $\text{OCH}_3$ ). HRMS (ESI):  $m/z$  calcd for  $\text{C}_{30}\text{H}_{24}\text{NO}_4$   $[\text{M}]^+$  : 462.1700; found: 462.1696.

### 3.3 Synthesis of compound **35**



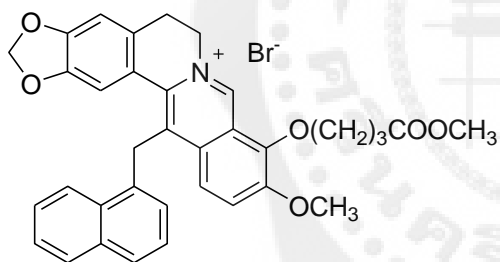
Compound **10** (50 mg, 0.11 mmol) and  $\text{K}_2\text{CO}_3$  (7.46 mg, 0.05 mmol) were dissolved in acetonitrile (2 mL) and then *tert*-butyl bromoacetate (0.1 mL, 0.68 mmol) was added. The reaction was refluxed at 80 °C for 5h. After the reaction complete, the mixture was concentrated and chromatographed on silica gel (2 % MeOH in DCM) to give compound **35** (32 mg, 45 %) as a yellow solid.  $^1\text{H}$  NMR ( $\text{CD}_3\text{OD}/\text{CDCl}_3$ ):  $\delta$  10.195 (s, 1H, 8-H), 7.20-8.30 (m, 8H, naphthyl Ar-H, 1-H, 4-H, 11-H, 12-H), 6.75-6.90 (m, 3H, naphthyl Ar-H), 5.88 (s, 2H,  $\text{OCH}_2\text{O}$ ), 5.08 (s, 2H, 9- $\text{OCH}_2$ ), 5.02 (s, 2H,  $\text{CH}_2\text{-Ph}$ ), 4.89 (br s, 2H, 6-H), 3.98 (s, 3H, 10- $\text{OCH}_3$ ), 3.18 (br s, 2H, 5-H). HRMS (ESI):  $m/z$  calcd for  $\text{C}_{36}\text{H}_{34}\text{NO}_6$   $[\text{M}]^+$  : 576.2381; found: 576.2367.

3.4 Synthesis of compound **36****36**

Compound **10** (50 mg, 0.11 mmol) and  $K_2CO_3$  (7.46 mg, 0.05 mmol) were dissolved in acetonitrile (2 mL) and then *tert*-butyl 3-bromopropionate (0.1 mL, 0.60 mmol) was added. The reaction was refluxed at 80 °C for 5h.

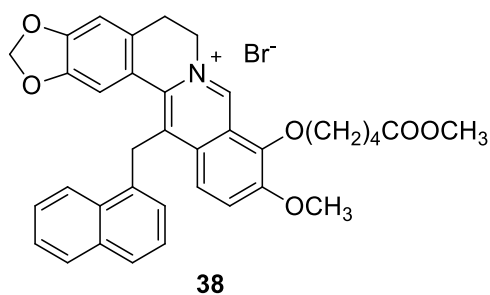
After the reaction complete, the mixture was

concentrated and chromatographed on silica gel (2 % MeOH in DCM) to give compound **36** (8.85 mg, 18 %) as a yellow solid.  $^1H$  NMR ( $CD_3OD/CDCl_3$ , 300 MHz):  $\delta_H$  10.54 (s, 1H, 8-H), 7.27- 8.13 (m, 8H, naphthyl Ar-H, 1-H, 11-H, 12-H), 6.83-6.99 (m, 3H, Ar-H, 4H), 5.85 (s, 2H,  $OCH_2O$ ), 5.22 (br s, 2H, H-6), 4.99 (s, 2H,  $CH_2$ -Ar), 4.75 (t,  $J = 6.0$  Hz, 2H, 9- $OCH_2$ ), 3.96 (s, 3H, 10- $OCH_3$ ), 3.31 (br s, 2H, 5-H), 3.06 (t,  $J = 6.0$  Hz, 2H,  $CH_2CO$ ), 1.487 (s, 9H,  $C(CH_3)_3$ ).

3.5 Synthesis of compound **37****37**

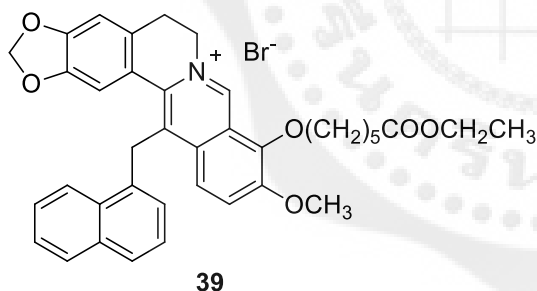
A mixture of compound **10** (50 mg, 0.11 mmol) and methyl 4-bromobutyrate (0.1 mL, 0.80 mmol) in dry  $CH_3CN$  (1 mL) was heated at 80 °C for 5 h under a nitrogen atmosphere. The mixture was then concentrated and chromatographed on silica gel (4% MeOH in DCM) to give **37** (25 mg, 40%) as a yellow

solid.  $^1H$  NMR ( $CD_3OD/CDCl_3$ ):  $\delta$  10.55 (s, 1H, 8-H), 7.27- 8.13 (m, 8H, naphthyl Ar-H, 1-H, 11-H, 12-H), 6.82-6.91 (m, 3H, Ar-H, 4H), 5.85 (s, 2H,  $OCH_2O$ ), 5.29 (br s, 2H, H-6), 4.98 (s, 2H,  $CH_2$ -Ar), 4.63 (t,  $J = 6.2$  Hz, 2H, 9- $OCH_2$ ), 3.93 (s, 3H,  $COOCH_3$ ), 3.62 (s, 3H, 10- $OCH_3$ ), 3.29 (br s, 2H, 5-H), 2.76 (t,  $J = 7.2$  Hz, 2H,  $OCH_2CH_2CH_2CO$ ), 2.36-2.41 (m,  $J = 6.8$  Hz, 2H,  $OCH_2CH_2CH_2CO$ ). HRMS (ESI):  $m/z$  calcd for  $C_{35}H_{32}NO_6$   $[M]^+$  : 562.2224; found: 562.2225.

3.6 Synthesis of compound **38**

A mixture of compound **10** (50 mg, 0.11 mmol) and methyl 5-bromovalerate (0.1 mL, 0.68 mmol) in dry  $\text{CH}_3\text{CN}$  (1 mL) was heated at  $80^\circ\text{C}$  for 5 h under a nitrogen atmosphere. The mixture was then concentrated and chromatographed on silica gel (4% MeOH in DCM) to give **38** (25 mg, 50%) as a

yellow solid.  $^1\text{H NMR}$  ( $\text{CD}_3\text{OD}/\text{CDCl}_3$ ):  $\delta$  10.51 (s, 1H, 8-H), 7.27- 8.13 (m, 8H, naphthyl Ar-H, 1-H, 11-H, 12-H), 6.82-6.91 (m, 3H, Ar-H, 4H), 5.85 (s, 2H,  $\text{OCH}_2\text{O}$ ), 5.29 (br s, 2H, H-6), 4.98 (s, 2H,  $\text{CH}_2\text{-Ar}$ ), 4.58 (t,  $J = 6.3$  Hz, 2H, 9- $\text{OCH}_2$ ), 3.66 (s, 3H,  $\text{COOCH}_3$ ), 3.94 (s, 3H, 10- $\text{OCH}_3$ ), 3.32 (br s, 2H, 5-H), 2.50 (t,  $J = 7.5$  Hz, 2H,  $\text{CH}_2\text{CO}$ ), 2.09-2.12 (m,  $J = 8.2$  Hz, 2H,  $\text{OCH}_2\text{CH}_2\text{CH}_2\text{CH}_2\text{O}$ ), 1.92-1.97 (m,  $J = 7.5$  Hz, 2H,  $\text{OCH}_2\text{CH}_2\text{CH}_2\text{CH}_2\text{O}$ ). HRMS (ESI):  $m/z$  calcd for  $\text{C}_{36}\text{H}_{34}\text{NO}_6$   $[\text{M}]^+$  : 576.2381; found: 576.2370.

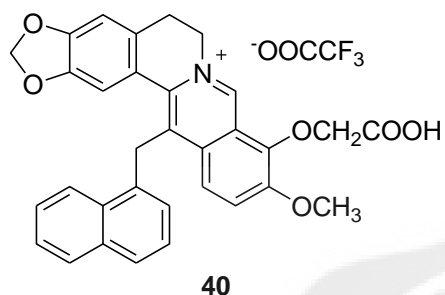
3.7 Synthesis of compound **39**

A solution of the 13-(1-naphthalenylmethyl) berberubine (20 mg, 0.043 mmol),  $\text{K}_2\text{CO}_3$  (3 mg, 0.023 mmol) and ethyl 6-bromoacetate (0.1 mL) in dry  $\text{CH}_3\text{CN}$  (1 mL) was heated at  $80^\circ\text{C}$  for 5 h under a nitrogen atmosphere. The reaction mixture was then concentrated and the

residue was chromatographed on silica gel (4% MeOH in DCM) to give **39** (10 mg, 38.46 %).  $^1\text{H NMR}$  ( $\text{CDCl}_3$ , 300 MHz):  $\delta$  10.47 (s, 1H, 8-H), 7.30- 8.11 (m, 8H, naphthyl Ar-H, 1-H, 11-H, 12-H), 6.84-6.90 (m, 3H, Ar-H, 4H), 5.85 (s, 2H,  $\text{OCH}_2\text{O}$ ), 5.30 (br s, 2H, H-6), 4.98 (s, 2H,  $\text{CH}_2\text{-Ar}$ ), 4.56 (t,  $J = 6.6$  Hz, 2H, 9- $\text{OCH}_2$ ), 3.94 (s, 3H, 10- $\text{OCH}_3$ ), 3.29 (br s, 2H, 5-H), 4.09 (q,  $J = 7.2$  Hz, 2H,  $\text{COCH}_2\text{CH}_3$ ), 2.37 (t,  $J = 7.05$  Hz, 2H,  $\text{OCH}_2\text{CH}_2\text{CH}_2\text{CH}_2\text{CH}_2\text{CO}$ ), 2.09-2.25 (m, 2H,  $\text{OCH}_2\text{CH}_2\text{CH}_2\text{CH}_2\text{CH}_2\text{CO}$ ), 1.60-1.91 (m, 2H,  $\text{OCH}_2\text{CH}_2\text{CH}_2\text{CH}_2\text{CH}_2\text{CO}$ ), 1.5-1.6 (m, 2H,

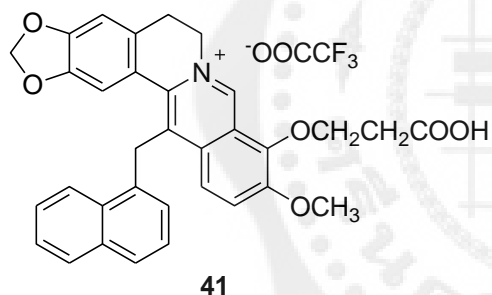
OCH<sub>2</sub>CH<sub>2</sub>CH<sub>2</sub>CH<sub>2</sub>CO), 1.24 (t, J = 7.05 Hz, 3H, COCH<sub>2</sub>CH<sub>3</sub>). HRMS (ESI): m/z calcd for C<sub>38</sub>H<sub>38</sub>NO<sub>6</sub> [M]<sup>+</sup> : 604.2693; found: 604.2659.

### 3.8 Synthesis of compound 40



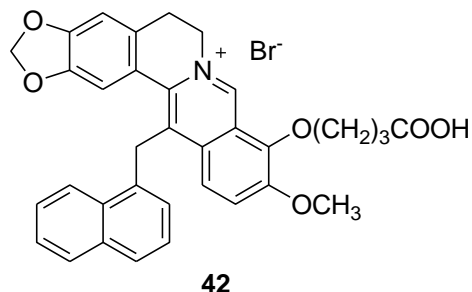
Compound **35** (10 mg, 0.02 mmol) was added trifluoroacetic acid (0.1 mL, mmol) in CH<sub>2</sub>Cl<sub>2</sub> (1 mL) and stirred at room temperature for 30 min. The reaction mixture was evaporated to dryness to give **40** (3 mg, 30% yield) as an orange solid. HRMS (ESI): m/z calcd for C<sub>32</sub>H<sub>26</sub>NO<sub>6</sub> [M]<sup>+</sup> : 520.1754; found: 520.1774.

### 3.9 Synthesis of compound 41

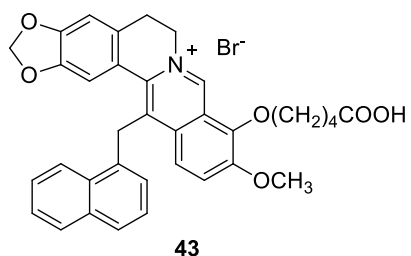


Compound **36** (10 mg, 0.02 mmol) was added trifluoroacetic acid (0.1 mL, xx mmol) in CH<sub>2</sub>Cl<sub>2</sub> (1 mL) and stirred at room temperature for 30 min. The reaction mixture was evaporated to dryness to give **41** (3 mg, 30%) as an orange solid. HRMS (ESI): m/z calcd for C<sub>33</sub>H<sub>28</sub>NO<sub>6</sub> [M]<sup>+</sup> : 534.1911; found: 534.1937.

### 3.10 Synthesis of compound 42

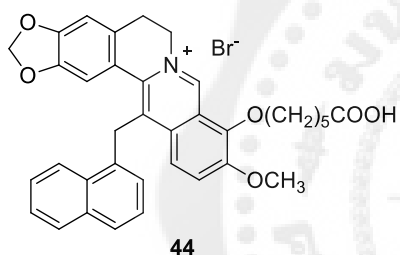


To a solution of compound **37** (20 mg, 0.04 mmol) in MeOH 1.2 mL was added 2% LiOH 0.5 mL. The solution was stirred at 70 °C for 5 h. The crude product was added to ice water (10 mL) and acidified to pH1 with 1M HCl. The mixture was then concentrated and chromatographed on C18-reversed phase silica gel (MeOH) to afford **42** (4 mg, 30%) as a yellow solid. HRMS (ESI): m/z calcd for C<sub>34</sub>H<sub>30</sub>NO<sub>6</sub> [M]<sup>+</sup> : 548.2067; found: 548.2088.

3.11 Synthesis of compound **43**

To a solution of compound **38** (20 mg, 0.04 mmol) in MeOH 1.2 mL was added 2% LiOH 0.5 mL. The solution was stirred at 70 °C for 5 hr. The mixture was then concentrated and chromatographed on C18-reversed phase silica gel (MeOH) to afford **42** (4 mg, 20%) as a yellow solid. HRMS (ESI): m/z calcd for

$C_{35}H_{32}NO_6$   $[M]^+$  : 562.2224; found: 562.2229.

3.12 Synthesis of compound **44**

To a solution of compound **39** (20 mg, 0.03 mmol) in MeOH 1.2 mL was added 2% LiOH 0.5 mL. The solution was stirred at 70 °C for 5 hr. The mixture was then concentrated and chromatographed on C18-reversed phase silica gel (MeOH) to afford **42** (3 mg, 15 %) as a yellow solid. HRMS (ESI): m/z calcd for

$C_{36}H_{34}NO_6$   $[M]^+$  : 576.2381 ; found: 576.2398.

## 4. Enzymes Activity

### 4.1 Phosphomevalonate kinase

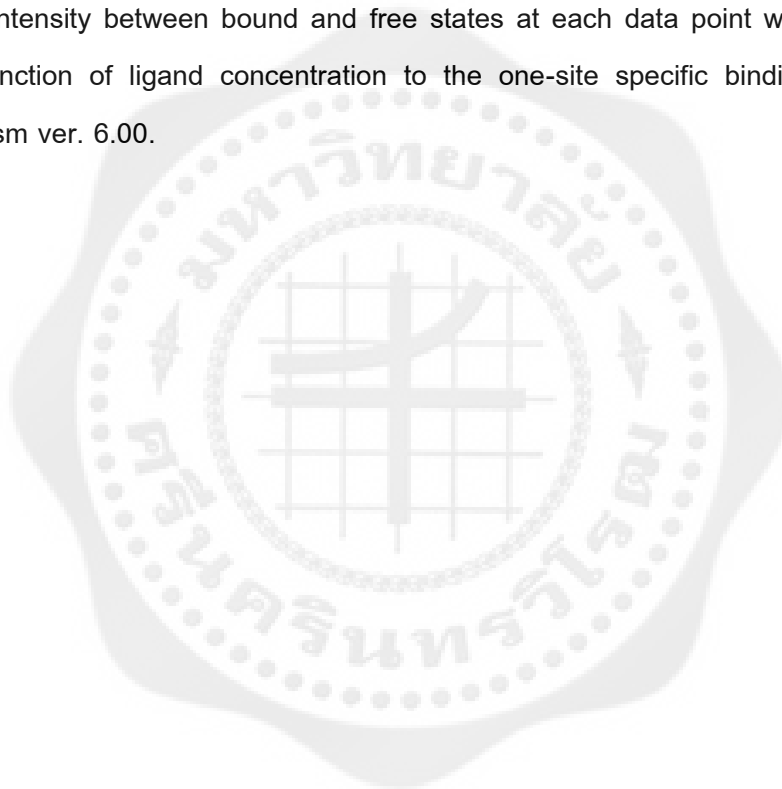
#### 4.1.1 Protein Expression and Purification

Human PMK is a 192-residue protein with a molecular weight of 22.0 kDa. To aid in purification, a hexa-histidine tag was added at the N-terminus resulting in a total molecular weight of 24.2 kDa. Human Phosphomevalonate kinase (PMK) pET15b expression plasmid was a gift from Henry Mizioro (Addgene plasmid # 52430). Briefly, the expression plasmid was transformed into *Escherichia coli* BL21 (DE3) Rosetta cells (Novagen) which encoded human PMK. Transformed bacteria were grown at 37 °C in Luria–Bertani (LB) medium containing ampicillin (amp). Then, cells were inoculated in 1 L of LB media containing amp. After that, protein expression was induced by adding 1 mM isopropyl- $\beta$ -D-thiogalactopyranoside (IPTG) when absorbance at 600 nm reached 0.6 at 600 nm. After 4 h of induction at 37 °C, cells were harvested by centrifugation for 30 minutes at 5000 rpm, re-suspended in a buffer containing 50 mM potassium phosphate, 5 mM imidazole, 5 % glycerol, 1 mM phenylmethanesulfonylfluoride (PMSF), and 300 mM NaCl at pH 7.8. Cells were lysed by passage through in a microfluidizer at 17 kpsi. The lysate was clarified by centrifugation at 13,000 rpm for 30 min, and the supernatant loaded onto 1 mL of a Ni-Sepharose Fast-Flow resin (GE Healthcare). The column was washed with the 50 mM phosphate buffer and the protein was gradient eluted using the same buffer supplemented with 5-300 mM imidazole. Protein concentration was determined spectrophotometrically using an extinction coefficient ( $\epsilon_{280}$ ) of 32,290 M<sup>-1</sup> cm<sup>-1</sup>. (Boonsri; et al. 2013: 313-319).

Protein was concentrated to 30  $\mu$ M by using a 10 kDa cutoff amicon ultra-15 centrifugal filter units and exchanged into a buffer containing 20 mM potassium phosphate, 100 mM potassium chloride, 5 mM DTT, 10 % glycerol, at pH 7.5. All synthesized compounds were dissolved in dimethyl sulfoxide (DMSO) to a concentration of 25 mM stock solution.

#### 4.1.2 Fluorescence measurements

Intrinsic fluorescence of the PMK enzyme bound to BBR derivatives were performed at 25 °C, using a SpectraMax M2 microplate readers. The fluorescence emission of human PMK was measured in 96-well plate with a total volume of 50  $\mu$ l of buffer solution containing 20 mM potassium phosphate, 100 mM potassium chloride, 10 % glycerol at pH 7.5 and 3.9  $\mu$ M PMK each well. Excitation was performed at 295 nm, and emission was recorded at 250–350 nm, and the spectra were recorded every 10 nm. To determine the  $K_d$  value, the difference in intensity between bound and free states at each data point were monitored and fitted as a function of ligand concentration to the one-site specific binding equation using GraphPad Prism ver. 6.00.



#### 4.2 The 3-Hydroxy-3-methyl-glutaryl-CoA Reductase Inhibition Assay

The commercially available HMGCR assay kit from Sigma-Aldrich, Catalog Number CS1090, was used to evaluate the HMGCR inhibition according to the manufacturer's instructions. The concentration of the purified human enzyme stock solution (Sigma) was 0.50 to 0.70 mg protein/mL. Reference statin drug, pravastatin, from Sigma was used as the positive control. To characterize HMGCR inhibition under defined assay conditions, reactions containing 4  $\mu$ L of NADPH and 12  $\mu$ L of HMG-CoA substrate in a final volume of 0.2 mL of 100 mM potassium phosphate buffer, pH 7.4, were initiated (Time 0) by the addition of 2  $\mu$ L of the catalytic domain of human recombinant HMGCR incubated in Bio Tek Synergy HT (Winooski, VT, USA) at 37 °C in the presence or absence (control) aliquots of the tested samples dissolved in DMSO. The blank experiment did not contain HMG-CoA reductase nor any of the studied substances. The rates of NADPH consumed were monitored every 20 s for up to 10 min by scanning spectrophotometrically. Two microliters were the amount of the sample used in the well. All measurements were done in triplicate. (Khazneh; et al. 2016: 404). The percentage of inhibition was calculated as follows:

$$\% \text{ inhibition} = \frac{\Delta A_{340} \text{ control} - \Delta A_{340} \text{ sample}}{\Delta A_{340} \text{ control}} \times 100\%$$

Table 3 Reaction volumes for 96 well plate samples.

Sample	1x Assay buffer	Inhibitor	NADPH	HMG-CoA	HMGCR
Blank	184 $\mu$ l	-	4 $\mu$ l	12 $\mu$ l	-
Activity	182 $\mu$ l	-	4 $\mu$ l	12 $\mu$ l	2 $\mu$ l
Inhibition	181 $\mu$ l	2 $\mu$ l for test compound 0.8 $\mu$ l for pravastatin	4 $\mu$ l	12 $\mu$ l	2 $\mu$ l

## CHAPTER 4

### RESULT AND DISCUSSION

On the basis of the SARs of berberine derivatives, the design of berberine derivatives by substitution with alkyl carboxylic group or alkyl ether group at C-9 using HMGR- and PMK-based computer-aided drug design was conducted. Molecular docking study of 24 structures of berberine derivatives to HMGR and PMK protein were successfully obtained with lower binding energy as compared to berberine. The results shown that substitution with alkyl carboxylic group (**11-15**) have lower binding energy than that of alkyl ether group (**16-34**). The binding energy increased with the length of aliphatic chain elongation as shown in Table 3.

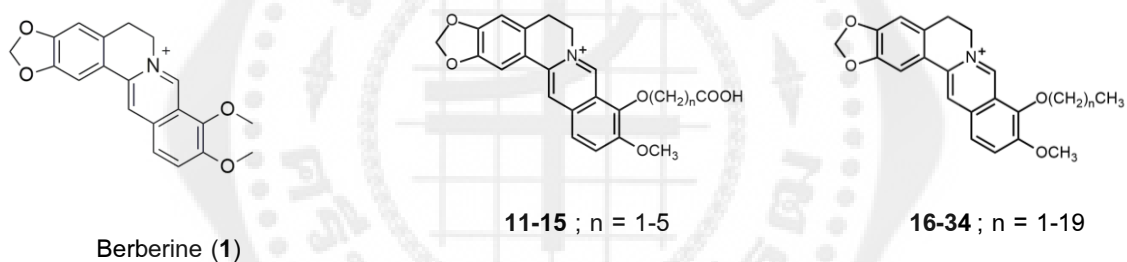


Figure 12 Structures of berberine and its derivatives where n is a number of methylene groups.

Table 4 Binding energy of berberine and its derivatives interacted to HMGCR and PMK based on molecular docking.

Compound	n	Binding energy (kcal/mol)	
		HMGCR	PMK
<b>Berberine (1)</b>	<b>0</b>	<b>-6.64</b>	<b>-6.66</b>
11	1	-8.5	-8.62
12	2	-9.26	-8.86
13	3	-9.3	-7.44
14	4	-9.13	-6.93
15	5	-8.63	-7.17
16	1	-6.76	-7.31
17	2	-6.48	-6.98
18	3	-6.63	-6.45
19	4	-6.84	-6.89
20	5	-7.2	-6.61
21	6	-7.7	-7.00
22	7	-7.32	-6.45
23	8	-7.16	-6.67
24	9	-7.61	-7.52
25	10	-6.81	-7.63
26	11	-6.8	-7.77
27	12	-7.09	-7.98
28	13	-6.59	-7.73
29	14	-6.81	-7.69
30	15	-7.61	-7.71
31	16	-7.09	-7.51
32	17	-7.01	-7.35
33	18	-6.73	-6.71
34	19	-6.66	-6.54

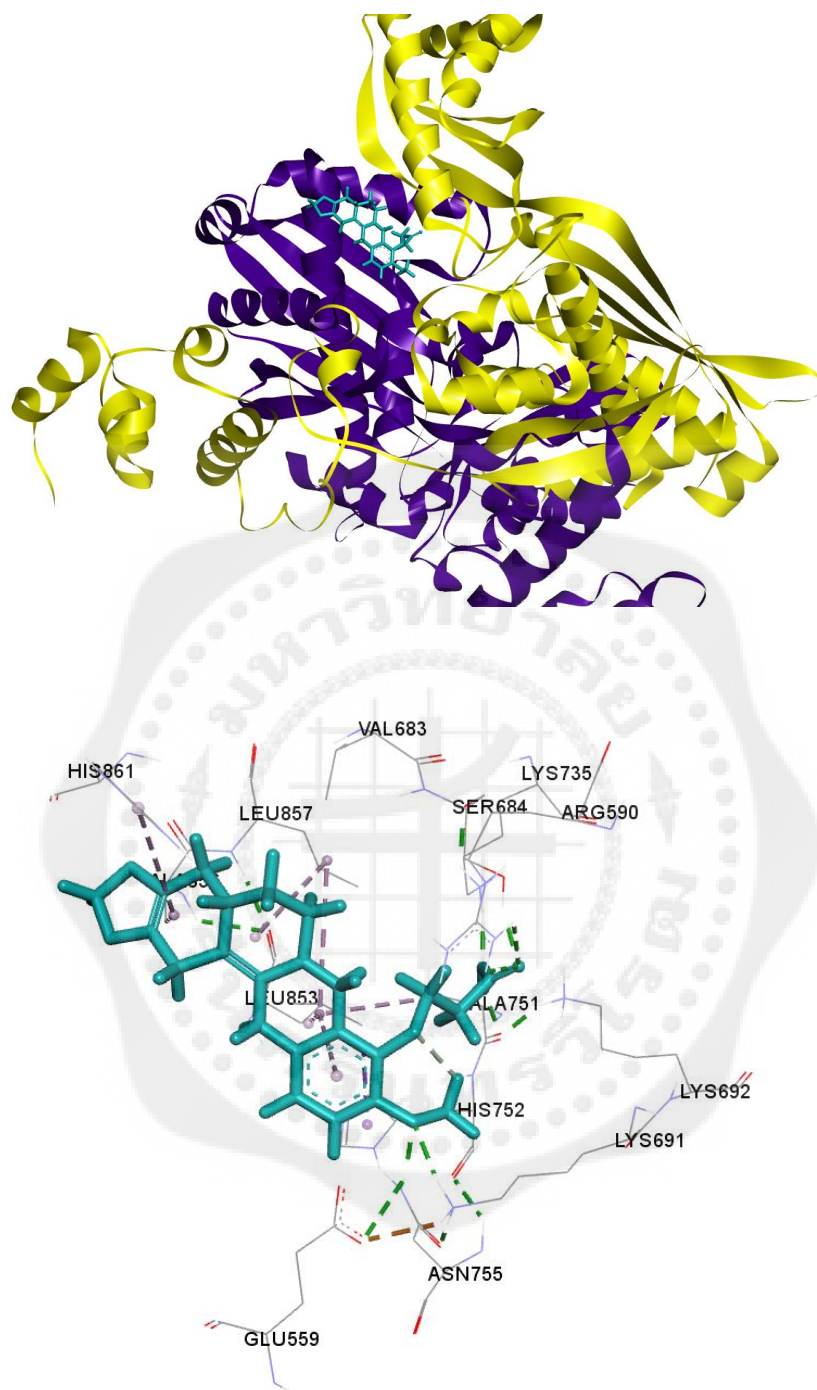


Figure 13 The three-dimensional model of of HMGCR bound to **12** were obtained from molecular docking (A), binding interactions of **12** to the human PMK active site from docking results (B).

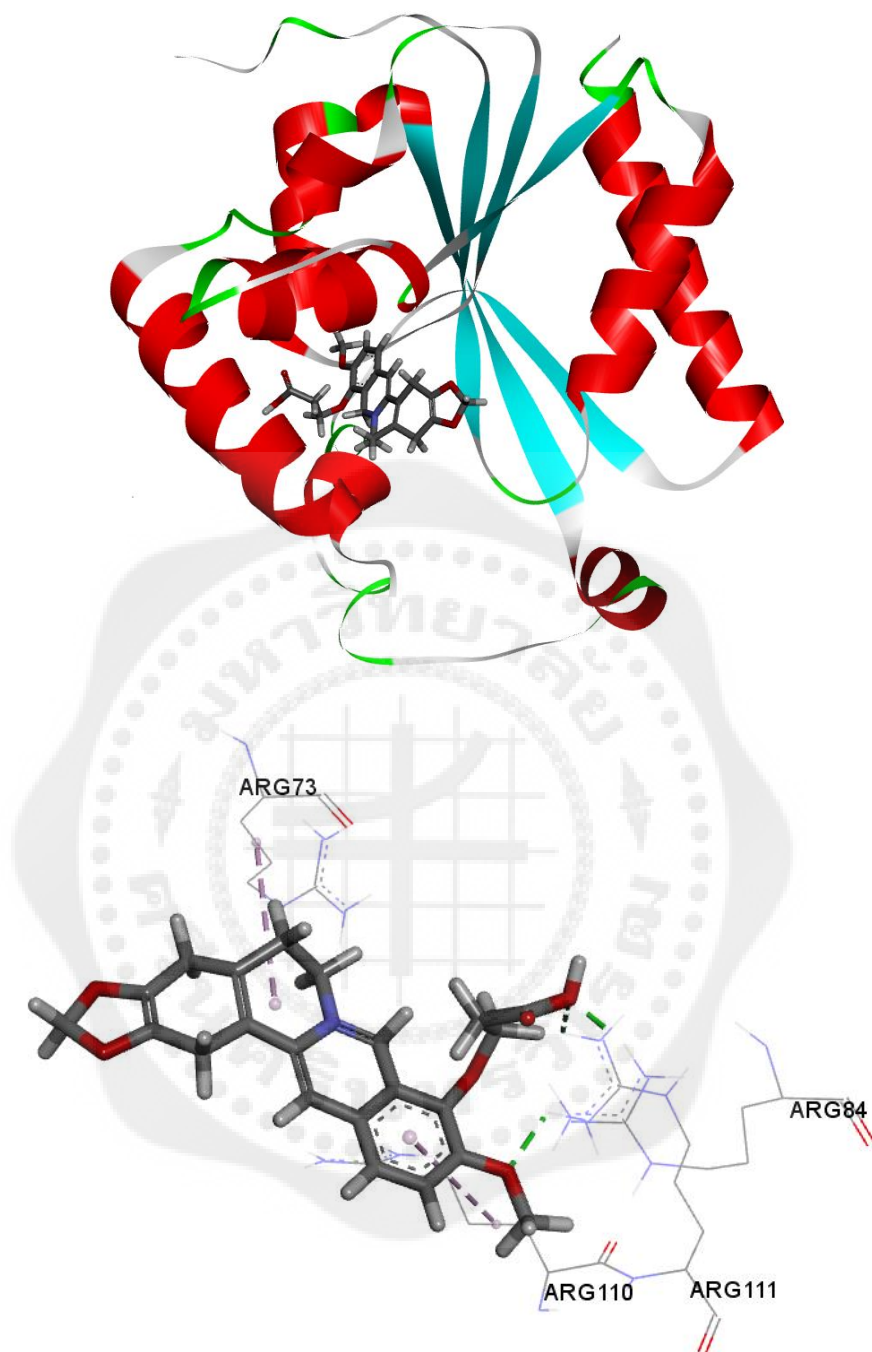


Figure 14 The three-dimensional model of of PMK bound to **12** were obtained from molecular docking (A), binding interactions of **12** to the human PMK active site from docking results (B).

From the previous molecular docking study, the results revealed that the predicted the alkoxy carboxylic derivatives **11-15** were more potent binding energies than the alkoxy derivatives **16-34**. Therefore, compounds **11-15** were chosen as the lead compounds for designing new potent dual action HMGCR and PMK inhibitors. In order to increase lipophilicity of compounds **11-15**, naphthalene moiety which contains in statin drud structure was designed to substitute at C-13 position of the compounds **11-15** to give compounds **35-44**. The binding energy of compounds **35-44** with both enzymes was shown in Table 4.

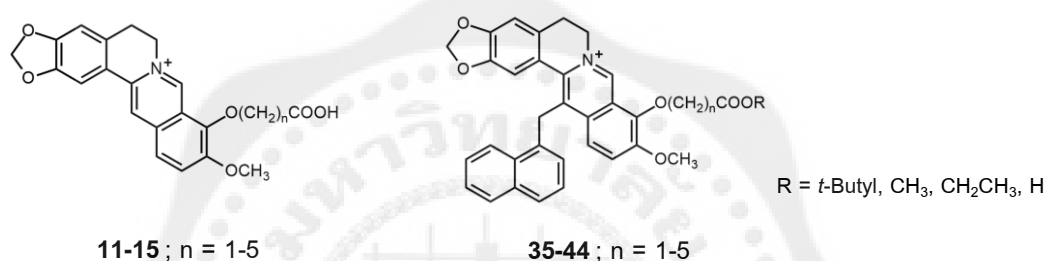


Figure 15 Structure of compounds **11-15** and **35-44** where n is a number of methylene groups.

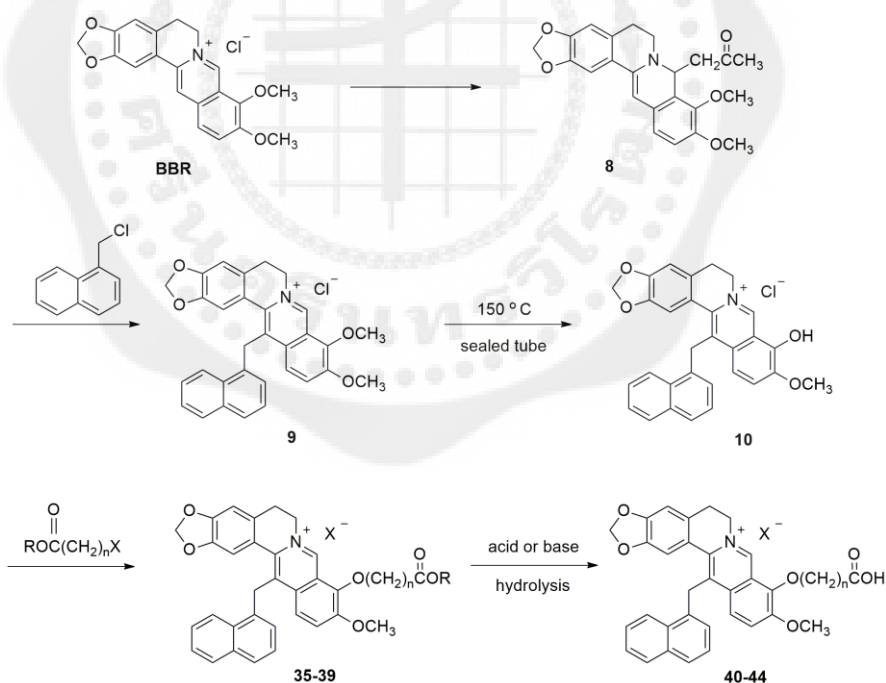
Table 5 Binding energy of the berberine derivatives (**35-44**) interacted to HMGCR and PMK based on molecular docking.

Compound	R	Binding energy (kcal/mol)	
		HMGCR	PMK
35	<i>t</i> -Butyl	-8.52	-7.51
36	<i>t</i> -Butyl	-8.46	-6.21
37	CH <sub>3</sub>	-9.03	-7.14
38	CH <sub>3</sub>	-8.96	-7.35
39	CH <sub>2</sub> CH <sub>3</sub>	-8.84	-5.14
40	H	-10.34	-6.12
41	H	-10.55	-8.28
42	H	-10.92	-7.69
43	H	-10.72	-7.96
44	H	-10.67	-8.27
Pravastatin	-	-8.89	-6.40

The results obtained from docking study provided valuable initial information about enzyme inhibitory activity (Table 4). Therefore, compounds **35-44** were chosen to be synthesized and evaluated their HMGR and PMK inhibitory activities.

### Synthesis

Twelve BBR derivatives were designed computationally and synthesized experimentally. The synthetic pathways involved 4 steps as shown in scheme 1. Treatment of BBR with acetone and sodium hydroxide gave an unstable 8-acetyldihydroberberine and subsequent alkylation with 1-(chloromethyl)naphthalene to yield **9** in 21%. Subsequently demethylation of **9** in DMF at 150 °C in sealed tube gave compound **10** in 42%, and then alkylation with corresponding alkylating agent to afford **35-39** in 17-50%. Finally hydrolysis with acid or base achieved the desired compounds **40-44** in yield of 15-30%.



Scheme 1 Synthesis pathway of the desired compounds **40-44**.

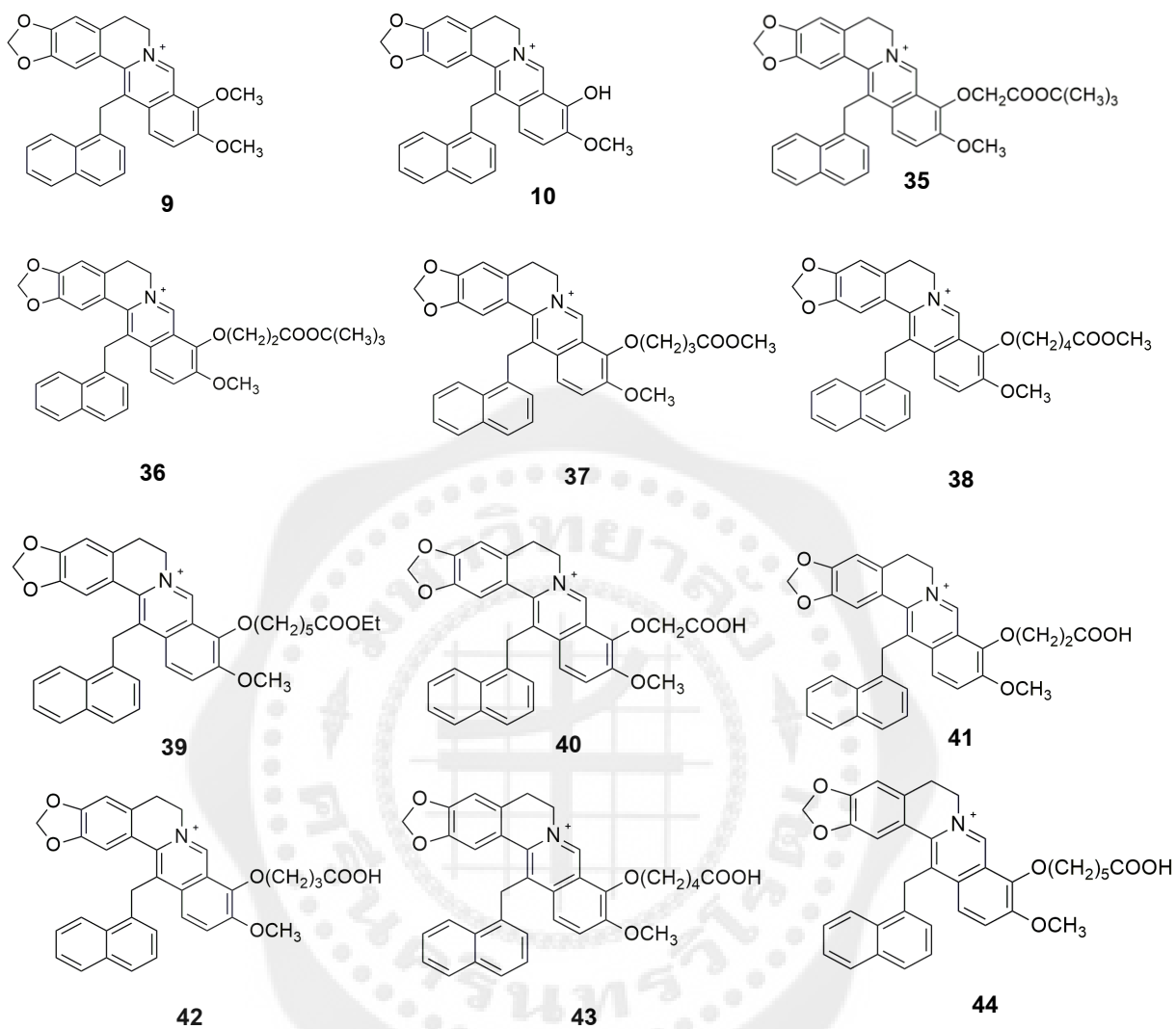


Figure 16 Structure of designed BBR derivatives.

Table 6 Reaction conditions and % yields for the synthesis of BBR derivatives (**35-39**)

Compound	mmol	Base/Reagent	mmol	Time (h.)	Product	n	% yield
<b>10</b>	0.11	K <sub>2</sub> CO <sub>3</sub>	0.05	5	<b>35</b>	1	45
		BrCH <sub>2</sub> COOC(CH <sub>3</sub> ) <sub>3</sub>	0.11				
<b>10</b>	0.11	K <sub>2</sub> CO <sub>3</sub>	0.05	5	<b>36</b>	2	18
		Br(CH <sub>2</sub> ) <sub>2</sub> COOC(CH <sub>3</sub> ) <sub>3</sub>	0.11				
<b>10</b>	0.11	K <sub>2</sub> CO <sub>3</sub>	0.05	5	<b>37</b>	3	40
		Br(CH <sub>2</sub> ) <sub>3</sub> COOCH <sub>3</sub>	0.11				
<b>10</b>	0.11	K <sub>2</sub> CO <sub>3</sub>	0.05	5	<b>38</b>	4	50
		Br(CH <sub>2</sub> ) <sub>4</sub> COOCH <sub>3</sub>	0.11				
<b>10</b>	0.043	K <sub>2</sub> CO <sub>3</sub>	0.023	5	<b>39</b>	5	38
		Br(CH <sub>2</sub> ) <sub>5</sub> COOCH <sub>2</sub> CH <sub>3</sub>	0.043				

### 1. Mannich Reaction

8-Acetyldihydroberberine (**8**) can be obtained by reaction of BBR with acetone in aqueous NaOH at 65°C, resulting in high yields of pale yellow solid (88%). This compound is an unstable product, therefore, it was then immediately alkylated in the next step without purification and characterization.

### 2. Enamine Alkylation

13-(1-naphthalenylmethyl)berberine (**9**) can be accessed by C-alkylation of 8-acetyldihydroberberine with 1-(chloromethyl)naphthalene at 80 °C to generate **9** in low yield (21%). The structure of **9** was confirmed by <sup>1</sup>H NMR spectroscopic analysis and mass spectrometry. The <sup>1</sup>H NMR revealed the presence of a signal assigned to H-8 proton next to an iminium salt at δ 10.97 as a singlet, and signals assigned to seven aromatic protons of naphthyl group at δ 7.20-8.10 were appeared. Moreover, none of acetyl group signals was

observed. The HRMS(ESI) showed a positive ion peak at  $m/z$  476.1856, which corresponded to the molecular ion of compound **9**.

### 3. Demethylation

13-(1-naphthalenylmethyl)berberubine (**10**) can be achieved by heating of **9** in DMF at 150°C. The resulting red solid of **10** was obtained in moderate yield (42 %). The structure of **10** was confirmed by  $^1\text{H}$  NMR spectroscopic analysis and mass spectrometry. The  $^1\text{H}$  NMR revealed the loss of one methoxy signal in the range of  $\delta$  3.8-4.2. The HRMS(ESI) showed a positive ion peak at  $m/z$  462.1696, which was consistent with the molecular ion of compound **10**.

### 4. O-Alkylation

13-(1-naphthalenylmethyl)-9-alkoxy ester derivatives **35-39** can be afforded by alkylation of **10** with corresponding alkylating agent in the presence of  $\text{K}_2\text{CO}_3$  at reflux. The yields were obtained in the range of 17-50 %. The  $^1\text{H}$  NMR spectrum of **35** revealed the presence of signal assigned to 9-OCH<sub>2</sub>-proton appeared at  $\delta$  5.08 as a singlet, and a signal attributed to nine protons of -C(CH<sub>3</sub>)<sub>3</sub> group appeared at  $\delta$  1.5 as a singlet. The ESIMS showed a positive ion peak at  $m/z$  576.24, which was consistent with the molecular ion of compound **35**. The  $^1\text{H}$  NMR spectrum of **36** also showed the presence of -C(CH<sub>3</sub>)<sub>3</sub> group appeared at  $\delta$  2.0, and two triplet signals attributed to two methylene protons of -OCH<sub>2</sub>CH<sub>2</sub>CO- group at  $\delta$  4.45 and 3.06. The  $^1\text{H}$  NMR spectra of **37-38** were almost the same as those for **36**, except for the methyl ester proton in the range of  $\delta$  3.6-3.9 as a singlet. The  $^1\text{H}$  NMR spectrum of **39**, the signal assigned to methylene protons were also similar to those for **36-38**. In addition, signals attributed to the ethyl ester group were observed at  $\delta$  4.29 and 1.24 as quartet and triplet, respectively. The HRMS(ESI) spectra showed a positive ion peak at  $m/z$  576.2367, 562.2225, 576.2370, 604.2659, which corresponded to the molecular ion of compound **36-39**, respectively.

## 5. Ester Hydrolysis

The hydrolysis of ester **35-36** was in acidic condition with TFA, while the hydrolysis of **37-39** was in basic condition with LiOH followed by acidified with HCl. The desired acids **40-44** were obtained in small amount after purification, which were confirmed by HRMS(ESI). No further work on structure characterization was undertaken due to time constraints.

Table 7 Reaction conditions and obtained % yields for the synthesis of BBR derivatives (**40-44**).

Compound	mmol	Reagent	mL	Time (h)	Product	n	% yield
<b>35</b>	0.017	TFA in	0.1	0.5	<b>40</b>	1	30
		CH <sub>2</sub> Cl <sub>2</sub>	1.0				
<b>36</b>	0.017	TFA in	0.1	0.5	<b>41</b>	2	30
		CH <sub>2</sub> Cl <sub>2</sub>	1.0				
<b>37</b>	0.035	2% LiOH in	0.5	5	<b>42</b>	3	30
		MeOH	1.2				
<b>38</b>	0.035	2% LiOH in	0.5	5	<b>43</b>	4	20
		MeOH	1.2				
<b>39</b>	0.016	2% LiOH in	0.25	5	<b>44</b>	5	15
		MeOH	0.6				

## Bioassays

### 1. Inhibitory activity of BBR derivatives againsts HMGCR

The inhibitory activity of BBR and its derivatives (**35-44**) were evaluated by using HMG-CoA reductase kits from Sigma-Aldrich, Catalog Number CS1090 according to the manufacturer's instructions. The results of the HMGCR inhibition assays of BBR and its derivatives are shown in Figure 17

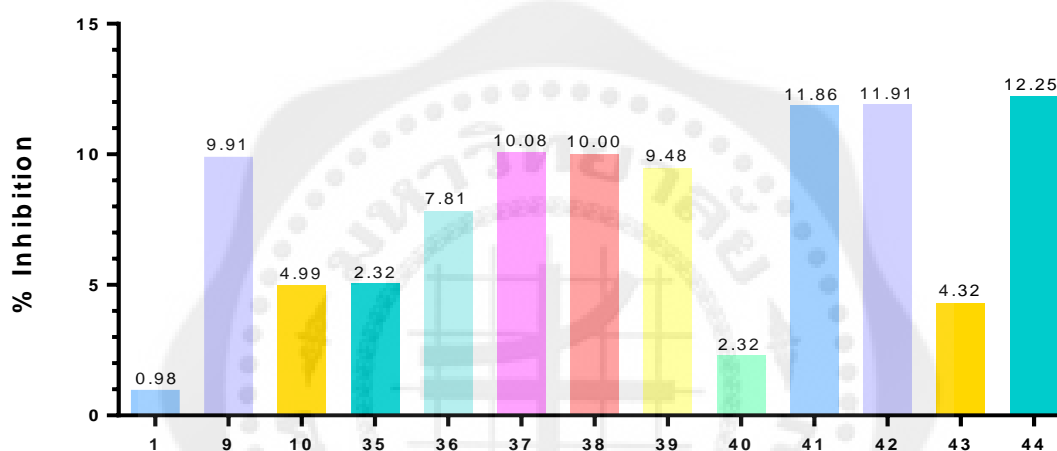
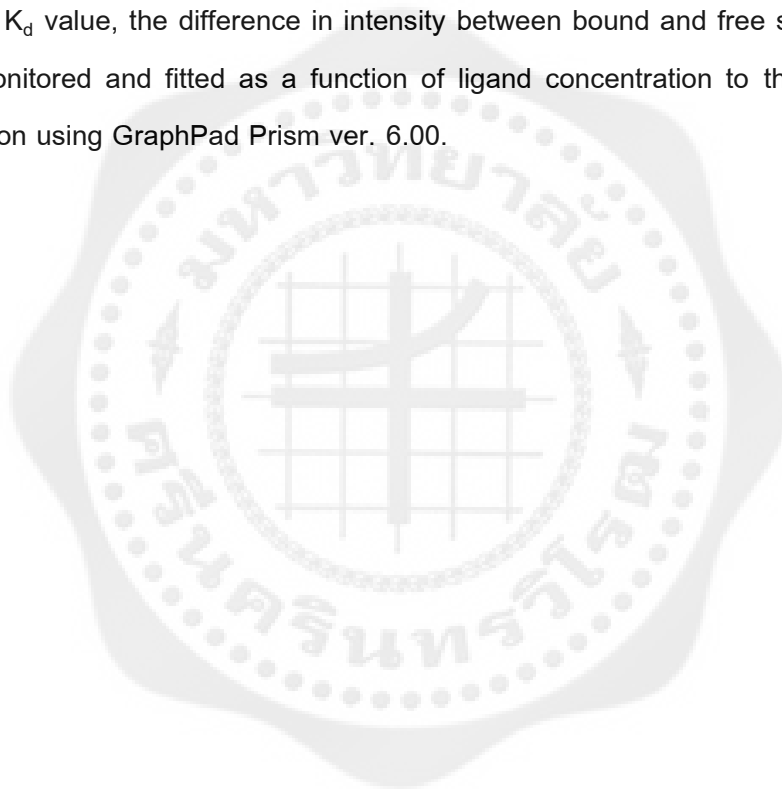


Figure 17 HMGCR percentage inhibition values for BBR and its derivatives (**9,10, 35-44**) at the same concentration of 10  $\mu$ M.

The results showed that the 13-naphthalenylmethyl BBR derivatives bearing 1-5 methylene groups at C-9 position were more potent than BBR. Among them, compound **41,42** and **44** showed the highest inhibition activity with percentage of inhibition around 12 at the same concentration with pravastatin drug (80.62% inhibition) and approximately 12-fold stronger inhibition than BBR (0.98% inhibition). The inhibitory activity of BBR derivatives was significantly strengthened when compared with BBR which the length of methylene group at C-9 position increased.

## 2. Binding affinity of BBR derivatives to phosphomevalonate kinase

Fluorescence measurements: Intrinsic fluorescence of the PMK enzyme bound to BBR derivatives were performed at 25 °C, using a SpectraMax M2 microplate readers. The fluorescence emission of human PMK was measured in 96-well plate with a total volume of 50  $\mu$ L of buffer solution containing 20 mM potassium phosphate, 100 mM potassium chloride, 10 % glycerol at pH 7.5 and 3.9  $\mu$ M PMK each well. Excitation was performed at 295 nm, and emission was recorded at 250–350 nm, and the spectra were recorded every 10 nm. To determine the  $K_d$  value, the difference in intensity between bound and free states at each data point were monitored and fitted as a function of ligand concentration to the one-site specific binding equation using GraphPad Prism ver. 6.00.



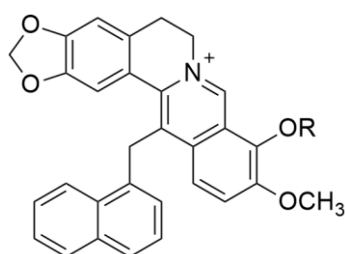


Figure 18 Core structure of BBR derivatives (35-44).

Table 8 Fluorescence study was used to experimentally verify binding affinity, and determine dissociation constants ( $K_d$  values).

Compound	R	$K_d$
BBR (1)	-	190.60 ± 17.86
9	CH <sub>3</sub>	103.70 ± 11.58
10	H	130.00 ± 35.35
35	CH <sub>2</sub> COOC(CH <sub>3</sub> ) <sub>3</sub>	70.76 ± 6.93
36	(CH <sub>2</sub> ) <sub>2</sub> COOC(CH <sub>3</sub> ) <sub>3</sub>	47.34 ± 2.83
37	(CH <sub>2</sub> ) <sub>3</sub> COOCH <sub>3</sub>	61.03 ± 3.87
38	(CH <sub>2</sub> ) <sub>4</sub> COOCH <sub>3</sub>	64.06 ± 8.99
39	(CH <sub>2</sub> ) <sub>5</sub> COOEt	117.40 ± 13.97
40	CH <sub>2</sub> COOH	100.10 ± 4.72
41	(CH <sub>2</sub> ) <sub>2</sub> COOH	64.77 ± 4.80
42	(CH <sub>2</sub> ) <sub>3</sub> COOH	85.09 ± 6.84
43	(CH <sub>2</sub> ) <sub>4</sub> COOH	74.92 ± 4.29
44	(CH <sub>2</sub> ) <sub>5</sub> COOH	110.10 ± 15.05

Understanding binding affinity is a key to appreciation of the intermolecular interactions driving biological processes, structural biology, and structure-activities relationships. It is also measured as part of the drug discovery process to help design drugs that bind their targets selectively and specifically. Binding affinity is typically measured and reported by the equilibrium dissociation constant ( $K_d$ ), which is used to evaluate and rank order strengths of bimolecular interactions. The smaller the  $K_d$  value, the greater the binding affinity of the ligand for its target. Binding affinity is influenced by non-covalent intermolecular interactions such as hydrogen bonding, electrostatic interactions, hydrophobic and Van der Waals forces between the two molecules. By inhibiting the cholesterol synthesis pathway, PMK enzyme was chosen as the protein target in this study. Thus, the lowest binding energy (BE) and the interactions of the BBR and its derivatives to the PMK were investigated based on docking studied. Screening of the designed BBR derivatives containing 12 derivatives for PMK inhibitor activity resulted in 7 compounds (**35-38** and **41-43**) which had greater inhibitory activity to that of BBR. Interestingly, all new designed BBR derivatives showed stronger binding interaction than the parent BBR. As the result, introduction of a naphthylmethyl group at C-13 position of BBR caused an increase in binding affinity. Substitution of methoxy group at C-9 position with alkoxy carboxylic group or alkoxy ester group showed better binding affinity with the  $K_d$  value in the range of 47.34 – 117.40  $\mu\text{M}$ . The obtained results indicated that the  $K_d$  value is decreased by increasing the length of methylene group at the C-9. It demonstrated that the increasing of hydrophobicity would be significantly enhanced the binding affinity.

### Cholesterol Lowering Agent Studies

Because it is difficult to completely inhibit one enzyme activity, inhibition of two sequential enzymes in the same pathway could be more effective than a single enzyme inhibition. In biosynthesis of cholesterol, HMGCR is the key enzyme to convert HMG-CoA to mevalonate, substance in mevalonate pathway, is an important metabolic pathway which plays a key role in multiple cellular processes by synthesizing sterol isoprenoids, such as cholesterol, and non-sterol isoprenoids. Phosphomevalonate kinase (PMK), catalyzes the rate-limiting step in isoprenoid/sterol biosynthesis, downstream of HMG CoA reductase. Hence HMGCR could be the main target to be represented as the good candidate for further study of the novel cholesterol lowering agent. From HMGCR activities, compounds **41** and **42** showed high potent percent inhibitory activity value in the range of 11.86 – 11.91 and approximately 12-fold more active than BBR (0.98 %inhibition). The obtained results agreed well to the binding affinity ( $K_d$ ) from PMK studies. Therefore these two compounds could be further developed as lead compound for inhibition of HMGCR and PMK activities.

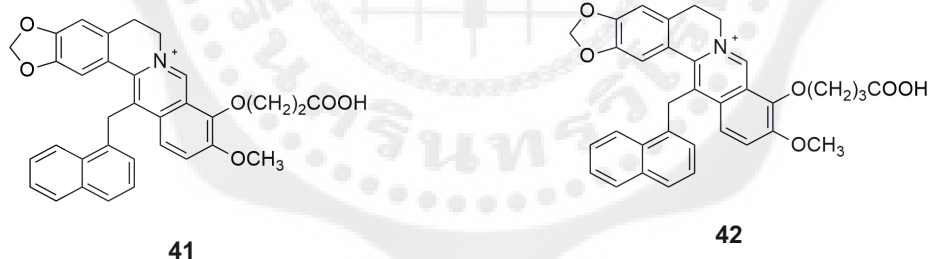


Figure 19 Structure of compound **41** and **42**.

From molecular docking, compound **41** was the best binding interaction to the human PMK at  $-8.28$  kcal/mol and the best  $K_d$  value of  $64.77 \pm 4.80$   $\mu$ M. Looking to the PMK active site, compound **41** showed the strong hydrogen bonding and more hydrophobic interactions than BBR (Figure 20). The obtained naphthalenylmethyl substituted at position 13 of compound **41** could enhance more hydrophobic interaction between the ligand and amino acids in the binding site as Lys19 residues and alkoxy carboxylic substituted at position 9 can interact with Ser154, Glu155 in active site of PMK with H-Bond. Consequently, the binding affinity of compound **41**, naphthalenylmethyl substituted at position 13 and alkoxy carboxylic substituted at position 9, to the human PMK showed the greatest than other molecules. Moreover, compound **42** showed similar mode of binding to PMK based on the obtained  $K_d$  and predicted binding energy.

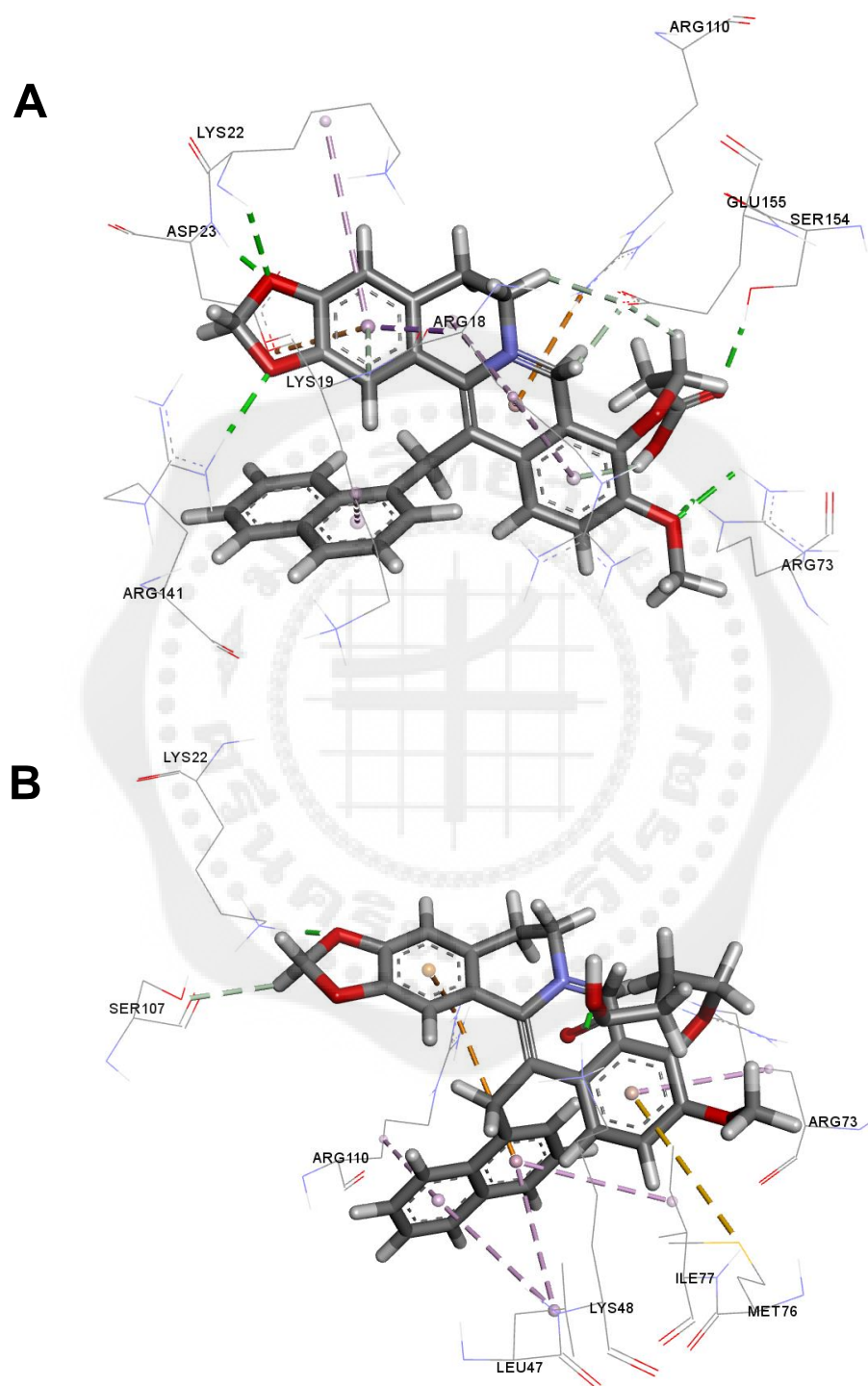
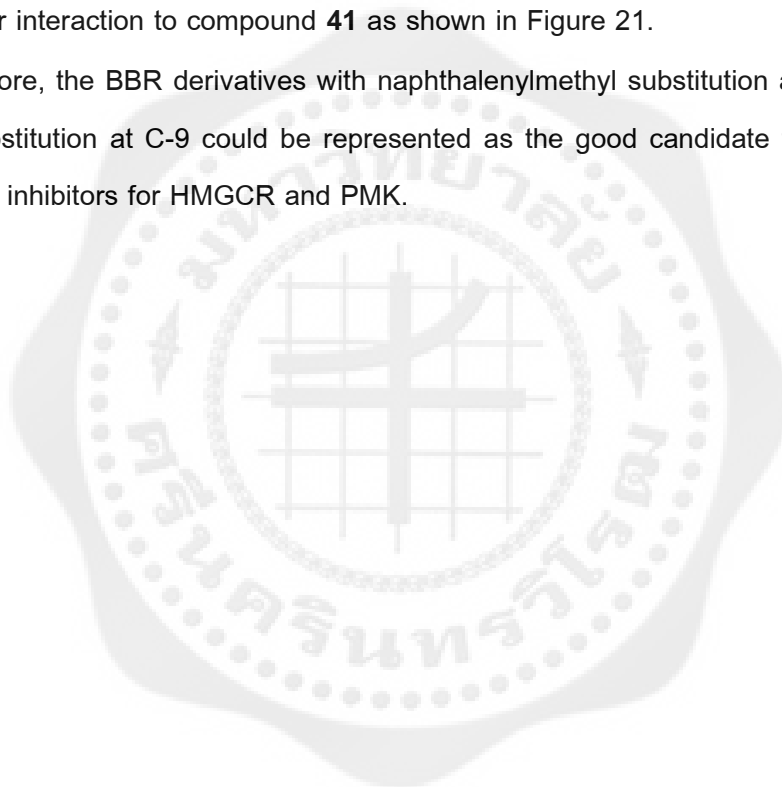


Figure 20 The binding interaction of compounds **41** (A) and **42** (B) with amino acids in active site of PMK.

In the active site of HMGCR, compound **41** had the lowest binding interaction at -10.55 kcal/mol and the highest inhibition activity with percentage of inhibition values was around 12. Considering interaction, alkoxy carboxylic substituted at position 9 showed the strong hydrogen bonding with the common amino acid in the cis-loop such as Ser684, Asp690, Lys691 and naphthalenylmethyl substituted at position 13 could enhance hydrophobic interaction with other residues including Arg590, Lys735, Ala751, His752, Leu853 and Cys561. Compound **42** also showed similar interaction to compound **41** as shown in Figure 21.

Therefore, the BBR derivatives with naphthalenylmethyl substitution at C-13 and alkoxy carboxylic substitution at C-9 could be represented as the good candidate for further study of the novel dual inhibitors for HMGCR and PMK.



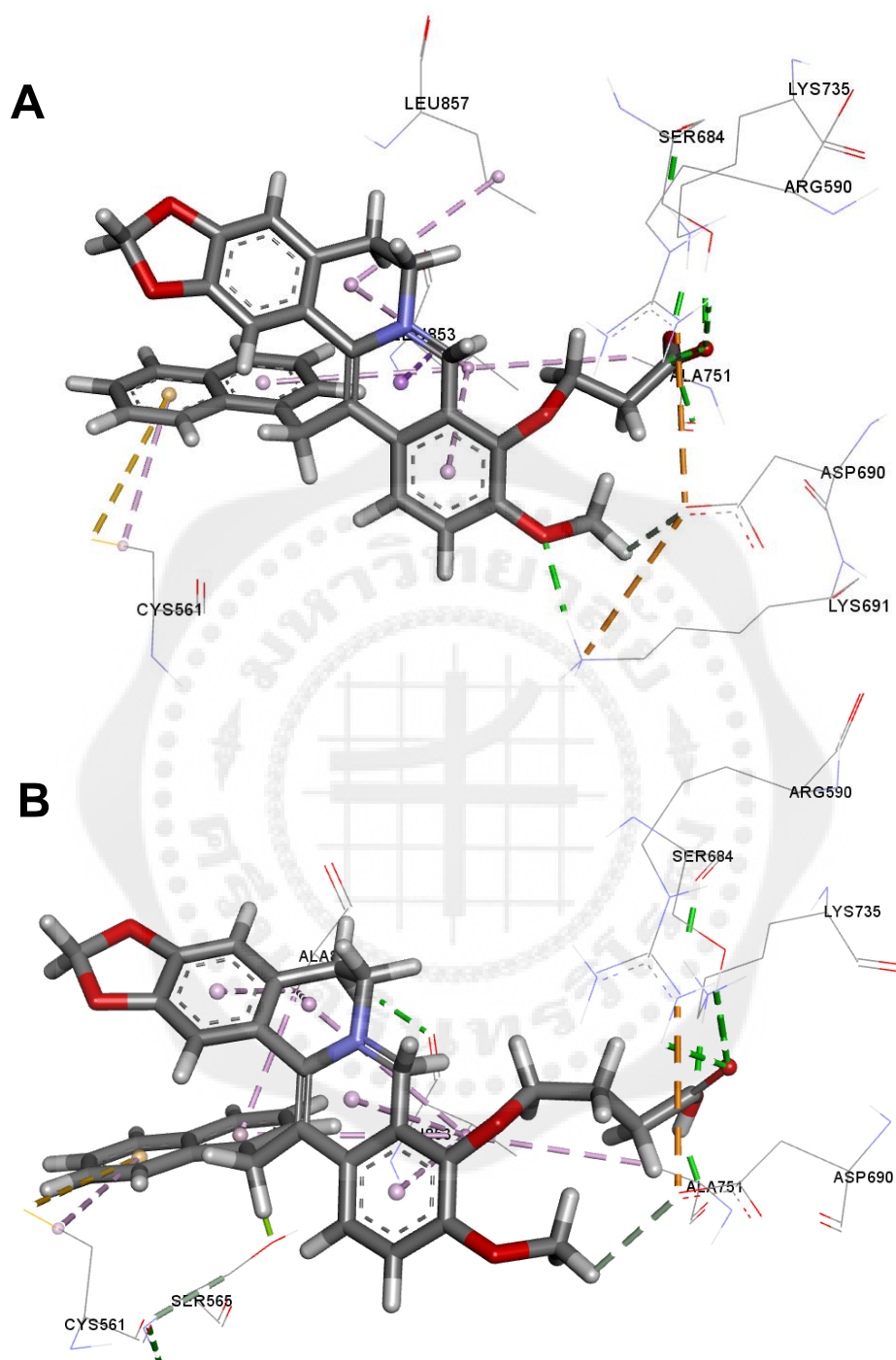


Figure 21 The binding interaction of compounds **41** (A) and **42** (B) with amino acids in active site of HMGCGR.

## CHAPTER 5

### CONCLUSION

In order to search for the new drugs modify from natural product as cholesterol-lowering activity against HMGCR and PMK enzymes, the 12 BBR derivatives were designed, synthesized and evaluated for their activities. Seven compounds (**35-38** and **41-43**) showed binding affinity with PMK better than their parent BBR with  $K_d$  values ranging from 47.34 to 80.09  $\mu\text{M}$ . Similarly to HMGCR, compounds **41,42** and **44** showed the highest inhibition activity with percentage of inhibition values in the range of 11.86-12.25 and approximately 12-fold more active than BBR (0.98 %inhibition). In this seires, compounds **41** and **42** were the best inhibitor for HMGCR with percentage of inhibition values of 11.86, 11.91, and PMK,  $K_d$  values of  $64.77 \pm 4.80$  and  $85.09 \pm 6.84$ , respectively. Therefore, compound **41** and **42**, naphthalenylmethyl substitution at C-13 and alkoxy carboxylic substitution at C-9, could be represented as the good candidate for further study of the novel HMGCR and PMK inhibitor.



**References**

## References

Argelles, N., Sanchez-Sandoval, E., Mendieta, A., Villa-Tanaca, L., Garduno-Siciliano, L., Jimenez, F., Cruz, M. d. C., Medina-Franco, J. L., Chamorro-Cevallos, G., Tamariz, J.

Design, synthesis, and docking of highly hypolipidemic agents: *Schizosaccharomyces pombe* as a new model for evaluating  $\alpha$ -asaronone-based HMG-CoA reductase inhibitors. *Bioorganic Med. Chem.* 2010, 18: 4238–4248.

Bitzur, R., Cohen, H., Kamari, Y., Harats, D. Intolerance to statins: Mechanisms and management. *Diabetes care.* 2013, 36: 2.

Boonsri, P., Neumann, T. S., Olson, A. L., Cai, S., Herdendorf, T. J., Miziorko, H. M., Hannongbua, S., Sem, D. S. Molecular docking and NMR binding studies to identify novel inhibitors of human phosphomevalonate kinase. *Biochem. Biophys. Res. Commun.* 2013, 430: 313–319.

Brusq, J. M., Ancellin, N., Grondin, P., Guillard, R., Martin, S., Saintillan, Y. Inhibition of lipid synthesis through activation of AMP kinase: an additional mechanism for the hypolipidemic effects of berberine. *J. Lipid. Res.* 2006, 47: 1281–1288.

Buhaescu, I., Izzedine, H. Mevalonate pathway: A review of clinical and therapeutical implication. *CLB.* 2007, 40: 575-584.

Cerqueira, N. M. F. S. A., Oliveira, E. F., Gesto, D. S., Diogo Santos-Martins., Moreira C., Moorthy, H. N., Ramos, M. J., Fernandes, P. A. Cholesterol biosynthesis: a mechanistic overview. *Biochemistry.* 2016, 55: 5483-5506.

Cicero, A. F., Rovati, L. C., Setnikar, I. Eulipidemic effects of berberine administered alone or in combination with other natural cholesterol-lowering agents. *A single-blind clinical investigation. Arzneimittelforsch.* 2007, 57, 26–30.

Dewick, P. Medicinal Natural Products: A Biosynthetic Approach (3 rd ed.). West Sussex, England Wiley. 2009, 357-388.

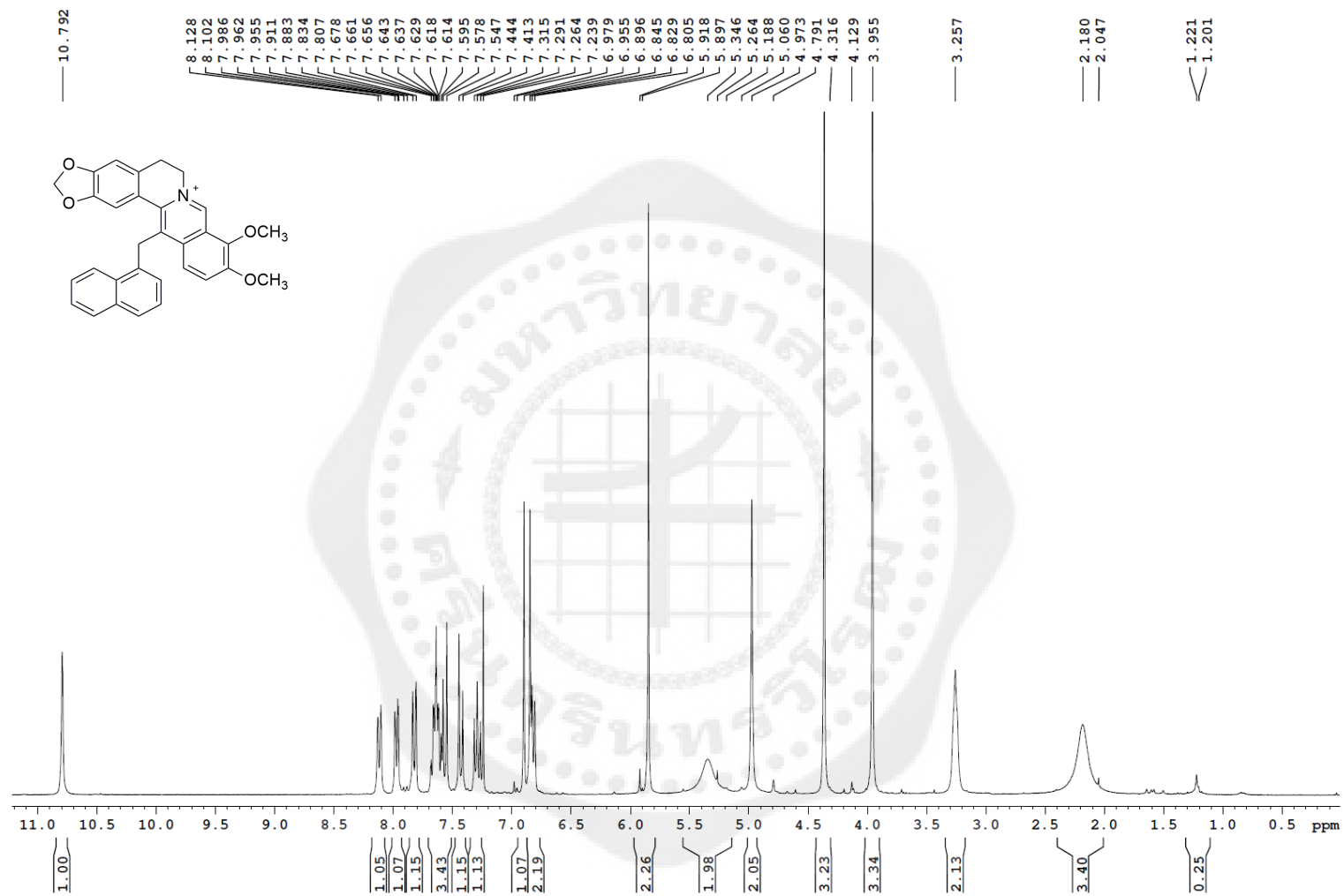
Endo, A., Kuroda, M., Tsujita, Y. ML-236A, ML-236B, AND ML-236C, New inhibitors of cholesterologenesis produced by penicillium citrinum. *J. Antibiot.* 1976A: 1346-1348.

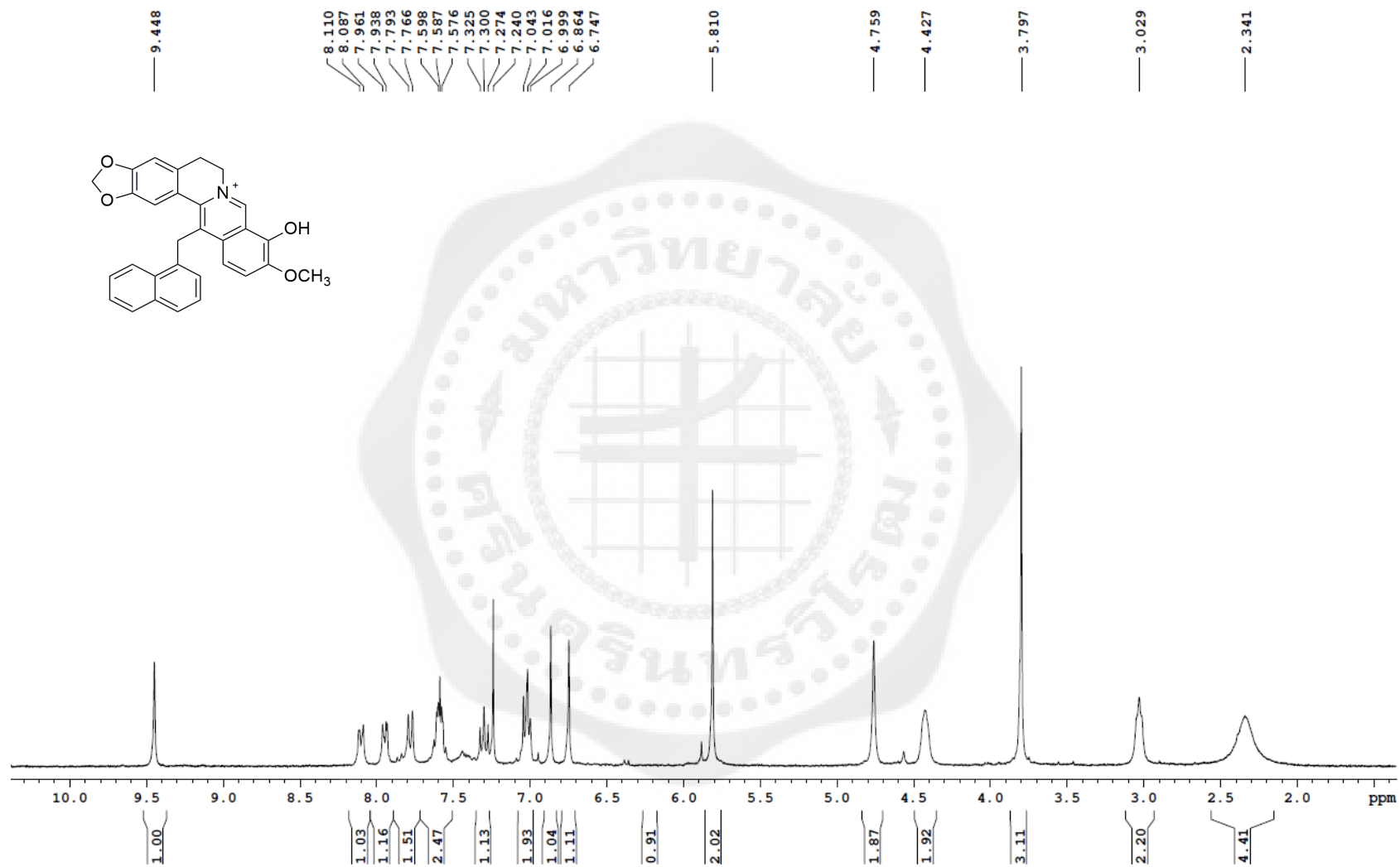
Endo, A., Kuroda, M., Tsujita, Y. Competitive inhibition of 3-hydroxy-3-ethylglutaryl coenzyme a reductase by ML-236A and ML-236B fungal metabolites, having hypocholesterolemic activity. *FEBS. Lett.* 1976B, 72: 323-326.

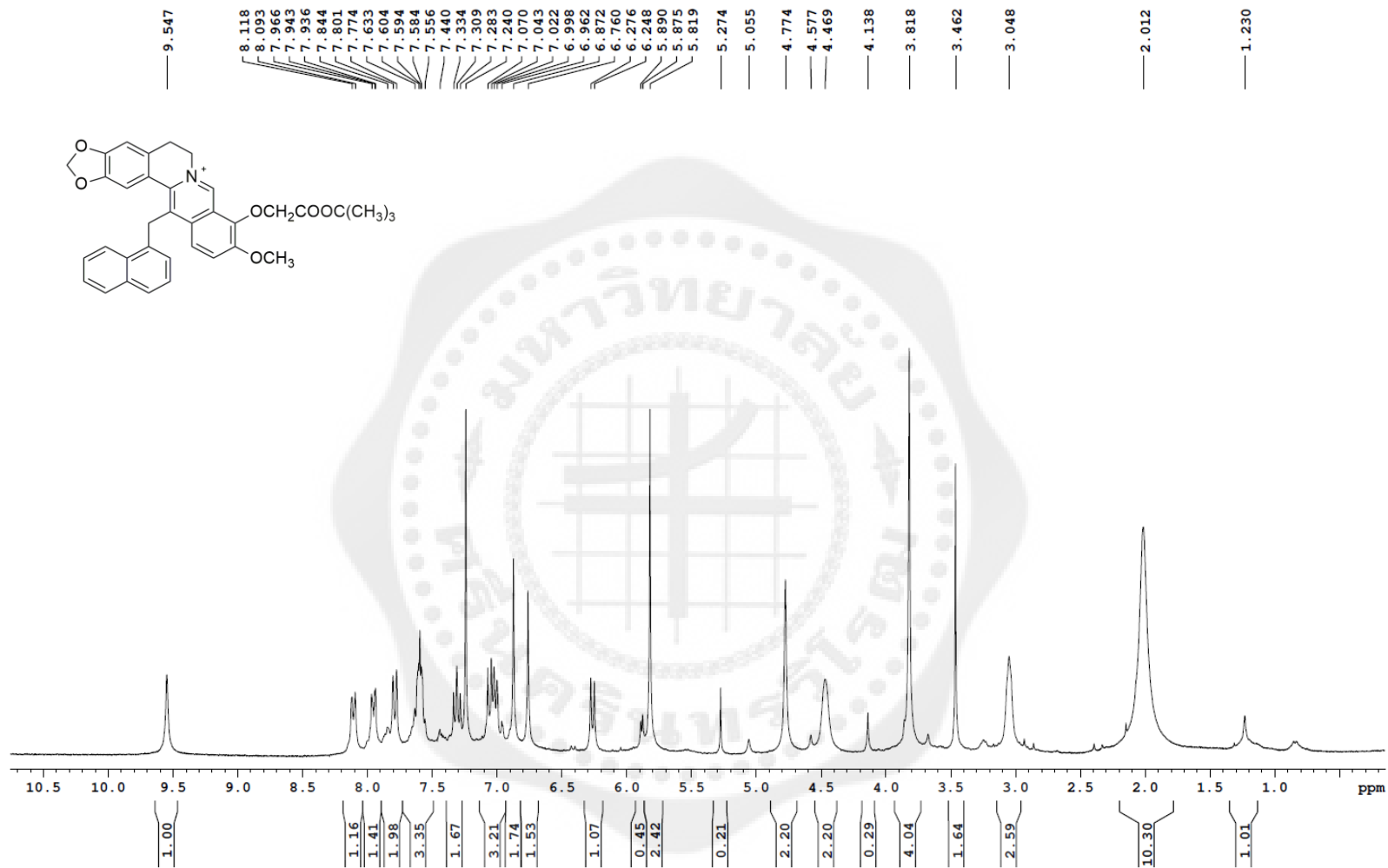
- Eyzaguirre, J., Valdebenito, D., Cardemil, E. Pig liver phosphomevalonate kinase: kinetic mechanism. *Arch. Biochem. Biophys.* 2006, 454: 190-196.
- Friesen, J. A., Rodwell, V. W. The 3-hydroxy-3-methylglutaryl coenzyme-A (HMG-CoA) reductases. *Genome Biol.* 2004, 5: 248.
- Khazneh, E., Hribova, P., Hosek, J., Suchy, P., Kollar, P., Prazanova, G., Muselik, J., Hanakova, Z., Vaclavik, J., Milek, M., Legath, J., Smejkal, K. The chemical composition of *achillea wilhelmsii* c. koch and its desirable effects on hyperglycemia, inflammatory mediators and hypercholesterolemia as risk factors for cardiometabolic disease. *Molecules.* 2016, 21: 404.
- Kong, W. J., Abidi, P., Lin, M., Inaba, S., Li, C., Wang, Y., Wang, Z., Si, S., Pan, H., Wang, S., Wu, J., Wang, Y., Li, Z., Liu, J., Jiang, J. D. Berberine is a novel cholesterol-lowering drug working through a unique mechanism distinct from statins. *Nat. Med.* 2004, 10: 1344–1351.
- Kong, W. J., Wei, J., Zuo, Z. Y., Wang, Y. M., Song, D. Q., You, X. F., Zhao, L. X., Pan, H. N., Jiang, J. D. Combination of simvastatin with berberine improves the lipid-lowering efficacy. *Metabolism.* 2008, 57: 1029–1037.
- Li, Y. H., Yang, P., Kong, W. J., Wang, Y. X., Hu, C. Q., Zuo, Z. Y., Wang, Y. M., Gao, H., Gao, L. M., Feng, Y. C., Du, N. N., Liu, Y., Song, D. Q., Jiang, J. D. Berberine analogues as a novel class of the low-density-lipoprotein receptor up-regulators: synthesis, structure-activity relationships, and cholesterol-lowering efficacy. *J. Med. Chem.* 2009, 52: 492–501.
- Mijares, A. H., Bañuls, C., Llopis, S. R., Morales, N. D., Lopez, I. E., Pablo, C. d., Alvarez, A., Veses, S., Rocha, M., Victor V. M. Effects of simvastatin, ezetimibe and simvastatin/ezetimibe on mitochondrial function and leukocyte/endothelial cell interactions in patients with hypercholesterolemia. *Atherosclerosis.* 2016, 247: 40-47.
- Pandey, M. K., Sung, B., Kunnumakkara, A. B., Sethi, G., Chaturvedi, M. M., Aggarwal, B. B. Berberine modifies cysteine 179 of I $\kappa$ B kinase, suppresses nuclear factor- $\kappa$ B-regulated antiapoptotic gene products, and potentiates apoptosis. *Cancer Res.* 2008, 68: 5370–5379.
- Singh, D. K., Banerjee, S., Porter, T. D. Green and black tea extracts inhibit HMG-CoA

- reductase and activate AMP kinase to decrease cholesterol synthesis in hepatoma cells. *J. Nutr. Biochem.* 2009, 20: 816–822.
- Silvaa, M. B. C., Souzaa, C. A. C., Philadelphoa, B. O., Cunhaa, M. M. N., Batistaa, F. P. R.,Silvaa, J. R., Druziana, J. L., Castilhoa, M. S., Cillib, E. M., Ferreira, E. S. In vitro and in silico studies of 3-hydroxy-3-methyl-glutaryl coenzyme A reductase inhibitory activity of the cowpea Gln-Asp-Phe peptide. *Food Chemistry.* 2018, 259: 270–277.
- Tang, L.Q., Wei, W., Chen, L. M., Sheng, L. Effects of berberine on diabetes induced by alloxan and a high-fat/high-cholesterol diet in rats. *J. Ethnopharmacol.* 2006, 108: 109–115.
- Wang, Y., Yi, X., Ghanam, K., Zhang, S., Zhao, T., Zhu, X. Berberine decreases cholesterol levels in rats through multiple mechanisms, including inhibition of cholesterol absorption. *Metabolism clinical and experimental.* 2014, 63: 1167-1177.
- Wei, G., ZHANG, Y., AI, L., QIAO, Y. Screening of HMG-CoA reductase inhibitors from composite salvia miltiorrhiza using autodock. *Chinese Journal of Natural Medicines.* 2010, 8(1): 0051-0056.
- Xiao, H. B., Sun, Z. L., Zhang, H. B., Zhang, D. S. Berberine inhibits dyslipidemia in C57BL/6 mice with lipopolysaccharide induced inflammation. *PHARMACOL REP.* 2012, 64: 889-895.
- Ye, X., He, K., Zhu, X., Zhang, B., Chen, X., Yi, J., Li, X. Synthesis and antihyperlipidemic efficiency of berberine-based HMG-CoA reductase inhibitor. *Med. Chem. Res.* 2012, 21: 1353–1362.
- Zeng, X. H., Zeng, X. J., Li, Y. Y. Efficacy and safety of berberine for congestive heart failure secondary to ischemic or idiopathic dilated cardiomyopathy. *Am. J. Cardiol.* 2003, 92: 173–176.
- Zhao, W., Xue, R., Zhou, Z .X., Kong, W .J., Jiang, J .D .Reduction of blood lipid by berberine in hyperlipidemic patients with chronic hepatitis or liver cirrhosis. *Biomed. Pharmacother.* 2008, 62: 730–731.

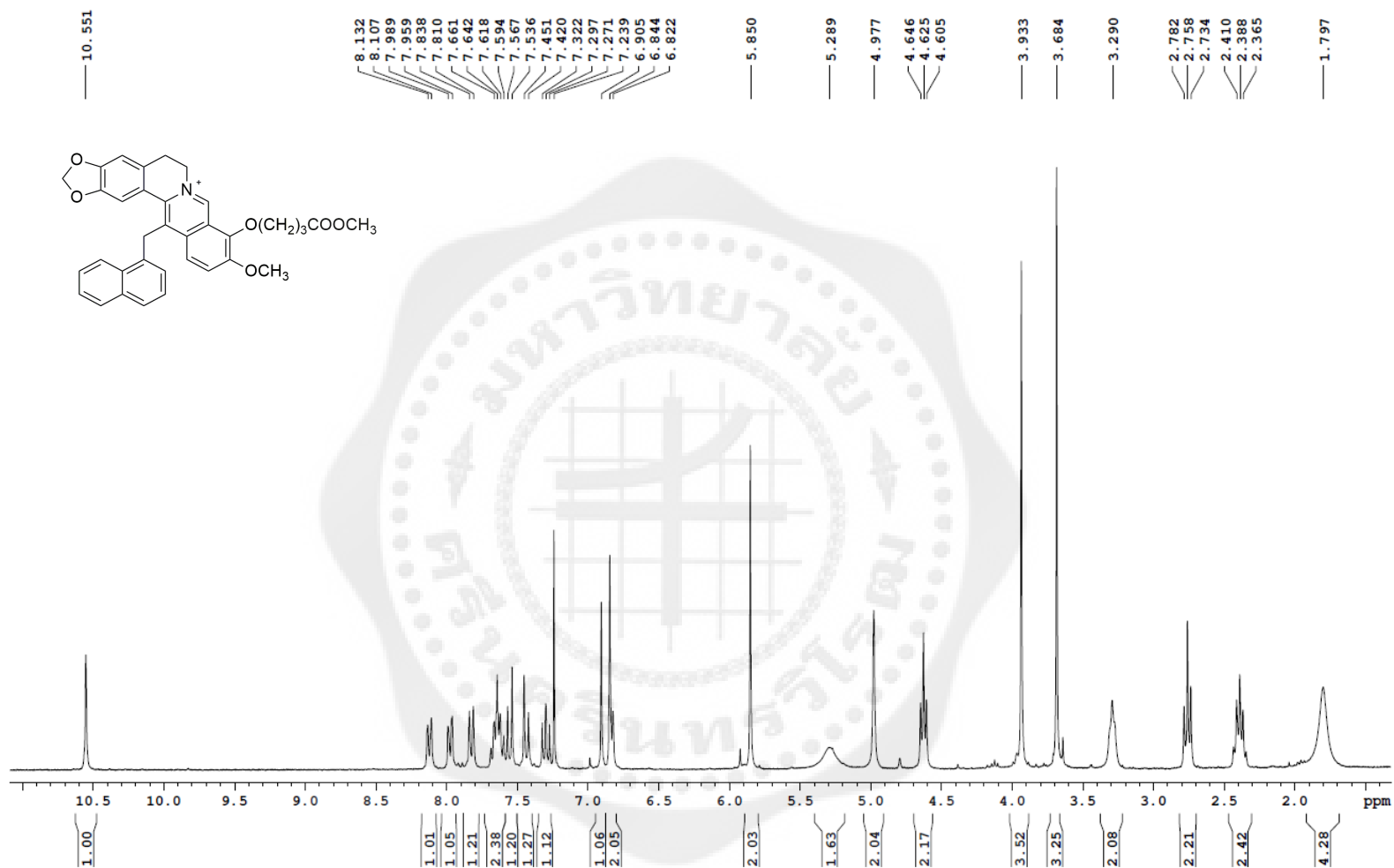


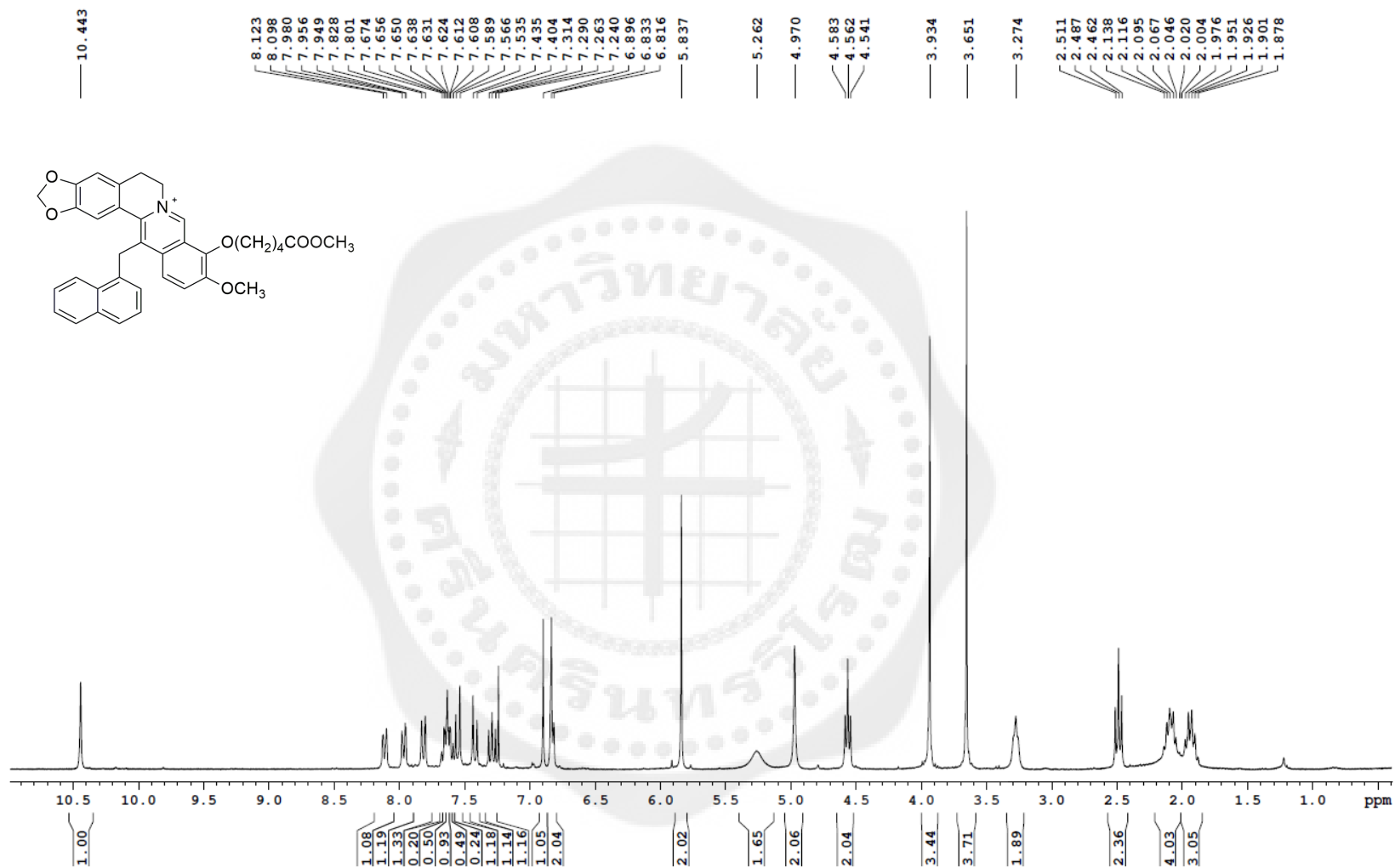
Figure 22 <sup>1</sup>H-NMR of compound **9** in CDCl<sub>3</sub>

Figure 23  $^1\text{H-NMR}$  of compound 10 in  $\text{CDCl}_3$

Figure 24  $^1\text{H-NMR}$  of compound **35** in  $\text{CDCl}_3$



Figure 26 <sup>1</sup>H-NMR of compound **37** in CDCl<sub>3</sub>

Figure 27 <sup>1</sup>H-NMR of compound **38** in CDCl<sub>3</sub>

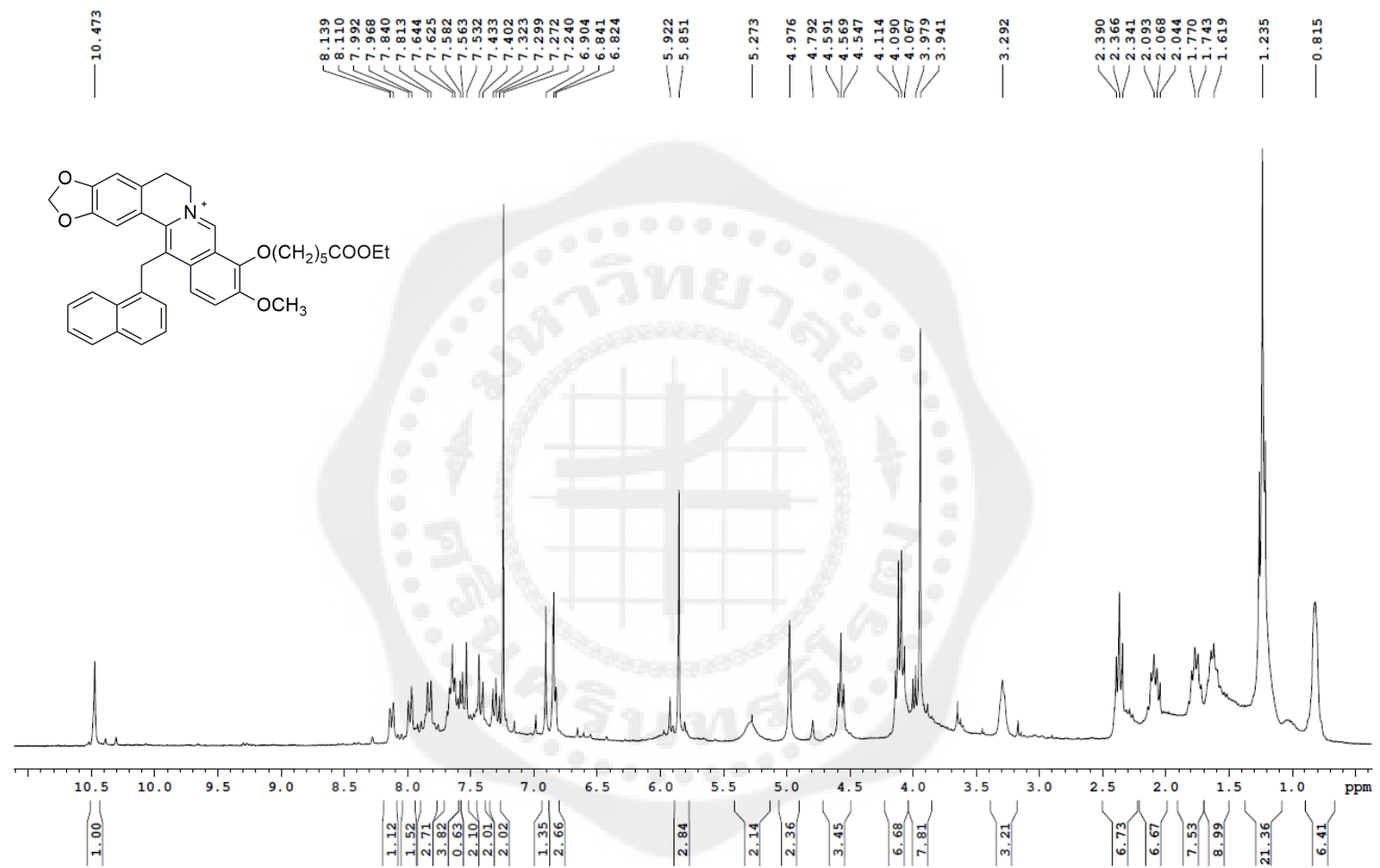
Figure 28 <sup>1</sup>H-NMR of compound **39** in CDCl<sub>3</sub>

Table 9 Fluorescence study was used to experimentally verify binding, and determine dissociation constants ( $K_d$  values).

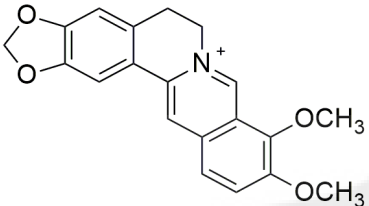
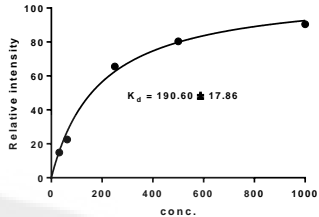
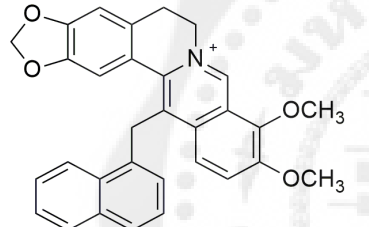
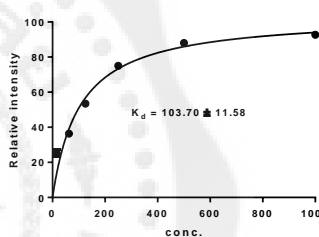
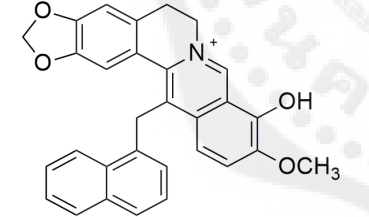
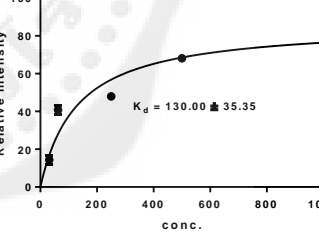
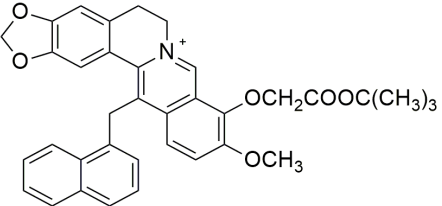
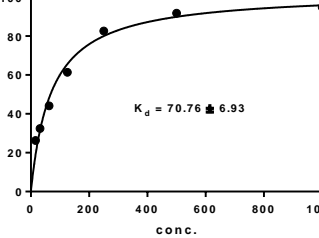
Structure	$K_d$ ( $\mu\text{M}$ )
	
	
	
	

Table 9 Fluorescence study was used to experimentally verify binding, and determine dissociation constants ( $K_d$  values).

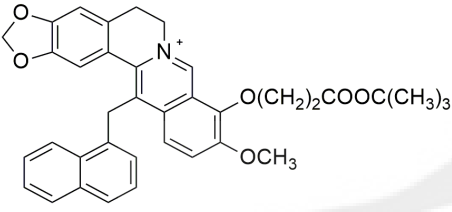
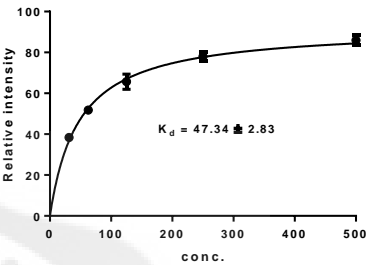
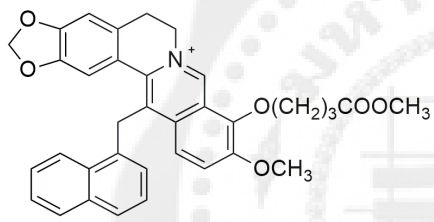
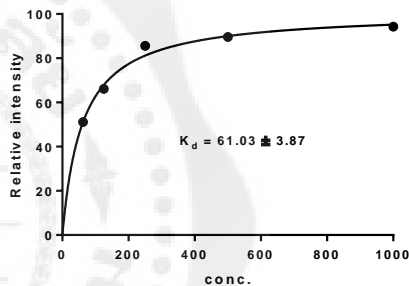
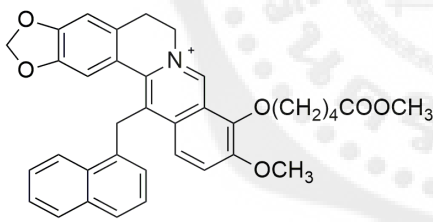
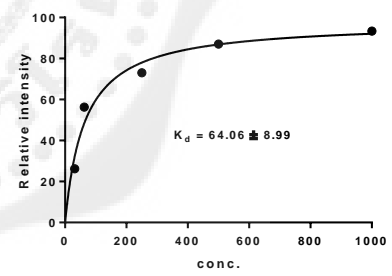
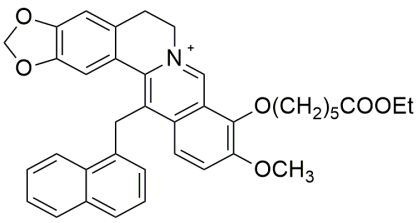
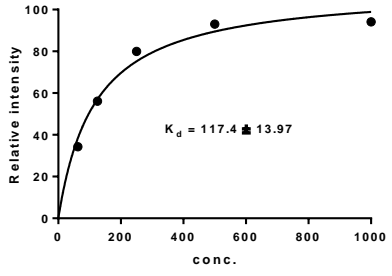
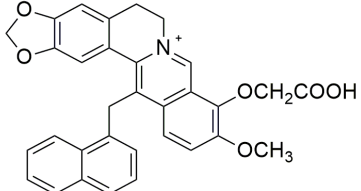
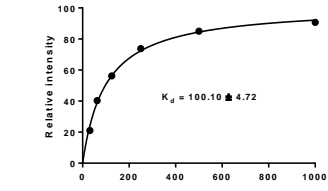
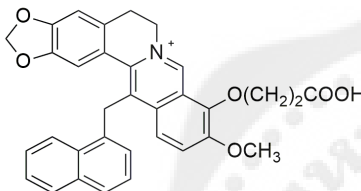
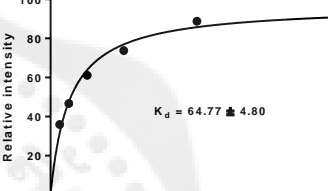
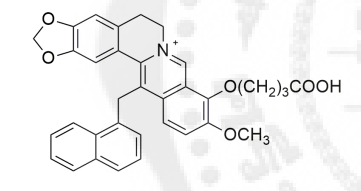
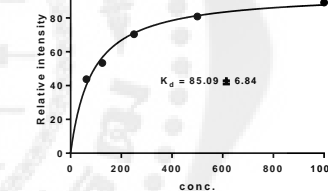
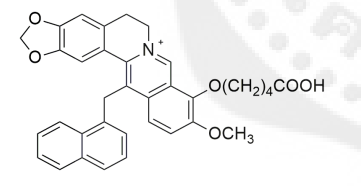
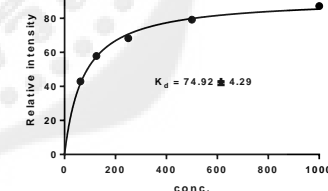
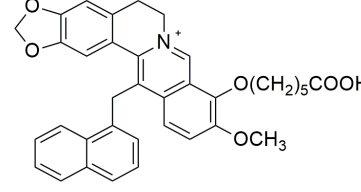
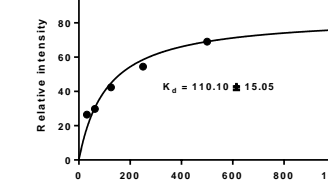
Structure	K <sub>d</sub> (μM)
	
	
	
	

Table 9 (continue)

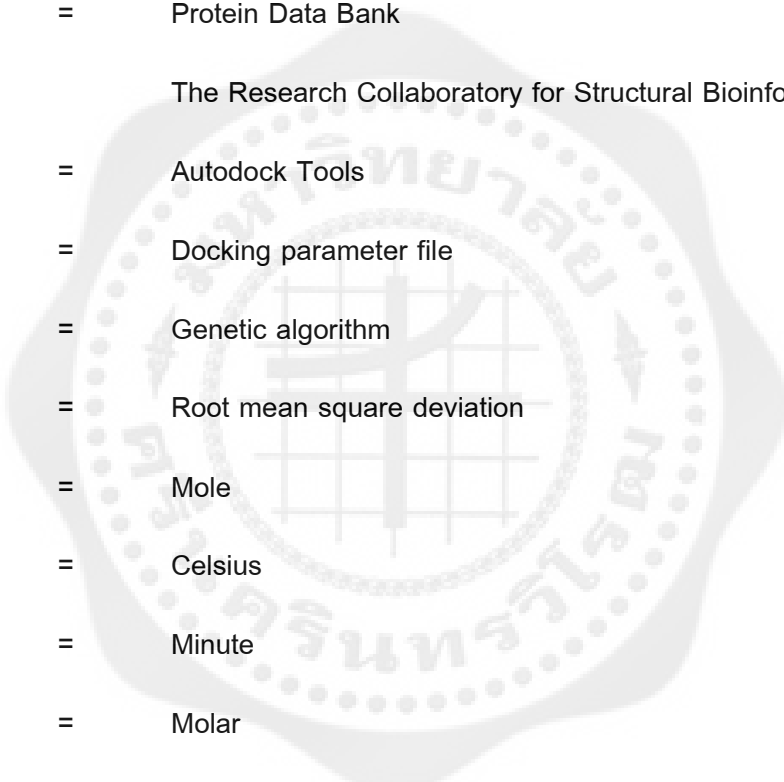
Structure	K <sub>d</sub> (μM)
	 <p><math>K_d = 100.10 \pm 4.72</math></p>
	 <p><math>K_d = 64.77 \pm 4.80</math></p>
	 <p><math>K_d = 85.09 \pm 6.84</math></p>
	 <p><math>K_d = 74.92 \pm 4.29</math></p>
	 <p><math>K_d = 110.10 \pm 15.05</math></p>



**GLOSSARY**

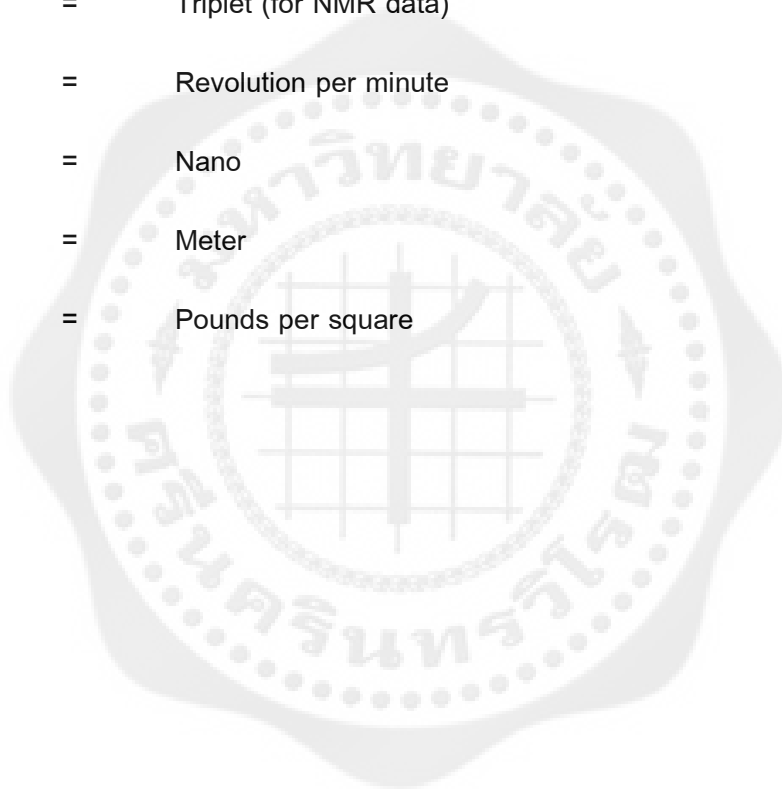
BBR	=	Berberine
HMG-CoA	=	3-hydroxy-3-methyl-glutaryl-CoA
HMGCR	=	3-hydroxy-3-methyl-glutaryl-CoA reductase
PMK	=	Phosphomevalonate kinase
ATP	=	Adenosine triphosphate
ADP	=	Adenosine diphosphate
M5P	=	Mevalonate-5-pyrophosphate
SARs	=	Structure activity relationship studies
LDLR	=	Low-density-lipoprotein receptor
Acetyl-CoA	=	Acetyl-coenzyme A
NADPH	=	Nicotinamide adenine dinucleotide phosphate
LDL	=	Low-density-lipoprotein
mRNA	=	Messenger ribonucleic acid
m	=	Milli
g	=	gram
TGs	=	triglycerides
LDL-c	=	LDL-cholesterol
HFHC	=	High-fat and high cholesterol
AMPK	=	AMP-activated protein kinase
SIMVA	=	Simvastatin
D	=	Day

LPS	=	Lipopolysaccharide
HDL-c	=	HDL-cholesterol
TC	=	Total cholesterol
LD <sub>50</sub>	=	Lethal dose 50 is the dose of a chemical which kills 50% of a sample population.
μ	=	Micro
Mol/L	=	Molar
IC <sub>50</sub>	=	The concentration of an inhibitor where the response (or binding) is reduced by half.
BBS	=	Berberine-baicalein
β	=	Beta
Ser	=	Serine
Lys	=	Lysine
CMS	=	Composite Salvia Miltiorrhiza
MDDR	=	MDL Drug Data Report
R <sup>2</sup>	=	Correlation coefficient
CF	=	Chloroform fraction
Da	=	Dalton
QDF	=	Glutamine-Aspartic acid-phenylalanine
k	=	Kilo
Arg	=	Arginine



$\alpha$	=	Alpha
$K_d$	=	Dissociation constants
$\Delta G$	=	Gibbs free energy
NMR	=	Nuclear magnetic resonance
Cal	=	Calorie
PDB	=	Protein Data Bank
RCSB		The Research Collaboratory for Structural Bioinformatics
ADT	=	Autodock Tools
dpf	=	Docking parameter file
ga	=	Genetic algorithm
RMSD	=	Root mean square deviation
mol	=	Mole
$^{\circ}\text{C}$	=	Celsius
min	=	Minute
M	=	Molar
$\delta$	=	Chemical shift
s	=	Singlet (for NMR data)
d	=	Doublet (for NMR data)
Hz	=	Hertz
J	=	coupling constant
m	=	Multiplet (for NMR data)

br	=	broad singlet (for NMR data)
HRMS (ESI)	=	High Resolution Electrospray Ionization Mass Spectrometry
m/z	=	Mass to charge ratio
h	=	Hour
Eq	=	Equivalent
t	=	Triplet (for NMR data)
rpm	=	Revolution per minute
n	=	Nano
m	=	Meter
psi	=	Pounds per square





## VITAE

Name Methachanun Jaitrong  
Date of Birth August 21, 1992  
Address 21/845 Sattahip District, Sattahip,  
Chonburi, Thailand

### Educational Background

2013 Bachelor of Science Degree in Chemistry  
Srinakharinwirot University, Bangkok, Thailand

2017 Master of Science Degree in Chemistry  
Srinakharinwirot University, Bangkok, Thailand